Observation of the Diurnal Cycle in the Low Troposphere of West Africa

Marie Lothon, Frédérique Saïd, Fabienne Lohou, Bernard Campistron

Observation of the Diurnal Cycle in the Low Troposphere of West Africa

MARIE LOTHON, FRÉDÉRIQUE SAÏD, FABIENNE LOHOU, AND BERNARD CAMPISTRON

Laboratoire d'Aérologie, Université de Toulouse, and CNRS UMR 5560, Toulouse, France

(Manuscript received 18 October 2007, in final form 5 March 2008)

ABSTRACT

The authors give an overview of the diurnal cycle of the low troposphere during 2006 at two different sites, Niamey (Niger) and Nangatchori (Benin). This study is partly based on the first observations of UHF wind profilers ever made in West Africa in the context of the African Monsoon Multidisciplinary Analysis (AMMA) project. Also used are the radiosoundings made in Niamey and ground station observations at Nangatchori, which allow for the study of the impact of the dynamics on the water vapor cycle and the turbulence observed at the ground.

Profiler measurements revealed a very consistent year-round nocturnal low-level jet maximal around 0500 UTC and centered at 400-m above the ground, with wind speed around 15 m s^{-1}. This jet comes either from the northeast during the dry season or from the southwest during the wet season, in relation with the position of the intertropical discontinuity. The radiosoundings made in Niamey highlight both the role of the nocturnal jet in bringing water vapor from the south during the night when the intertropical discontinuity has reached the vicinity of the considered area at the end of the dry season and the role of the daytime planetary boundary layer in mixing this water vapor within a larger depth of the troposphere. The planetary boundary layer processes play a large role in the diurnal cycle of the position of the intertropical discontinuity itself.

The observations of turbulence made at the ground in Nangatchori showed that the best signature of the nocturnal jet close to surface can be seen in the turbulent kinetic energy and skewness of the air vertical velocity, rather than on the mean wind itself. They reveal the downward transport of momentum from the jet core aloft to the surface.

1. Introduction

For the past 40 yr West Africa has experienced a strong rainfall deficit that induced drought periods and disastrous consequences on agricultural activities, economic development, and living conditions (Nicholson et al. 2000). In particular, the Sahelian zone (i.e., the southern sub-Saharan transition) appears as the world's most dramatic example of this long-term climatic change. For its water resources, West Africa is mainly dependent on the moisture transported inland from the Guinea Gulf by a monsoon system, the West African monsoon (WAM), which occurs from June to October during the boreal summer. Improvement of the knowledge and understanding of the mechanisms and interactions that control the WAM at different time and space scales was the primary objective of the African Monsoon Multidisciplinary Analysis (AMMA) launched in 2005 (Redelsperger et al. 2006, 2007). The present study is based on the data collected during the 2006 AMMA special observing campaign, where several hundred scientists and technicians and dozens of laboratories from different countries gathered during the 6-month period of the monsoon. The quadrilateral of the AMMA research domain can be roughly delimited to the north by the Tropic of Cancer, to the west by the African coast, to the south by the Guinea Gulf, and to the east by Niger–Nigeria border (Fig. 1).

In the annual cycle, the weather of this intertropical region is governed by the position and activity of the intertropical convergence zone (ITCZ) that follows the apparent latitudinal movement of the sun (Hastenrath 1995). This convergence and the differential surface heating between ocean and continent trigger and maintain the low-level humid monsoon flux from the Guinea Gulf. In opposition to the low-level southwesterly flow, a northeasterly advection (Harmattan) of a dry and

Corresponding author address: Marie Lothon, Laboratoire d'Aérologie, Centre de Recherches Atmosphériques, 8 route de Lannemezan, 65300 Campistrous, France.
E-mail: marie.lothon@aero.obs-mip.fr

DOI: 10.1175/2008MWR2427.1

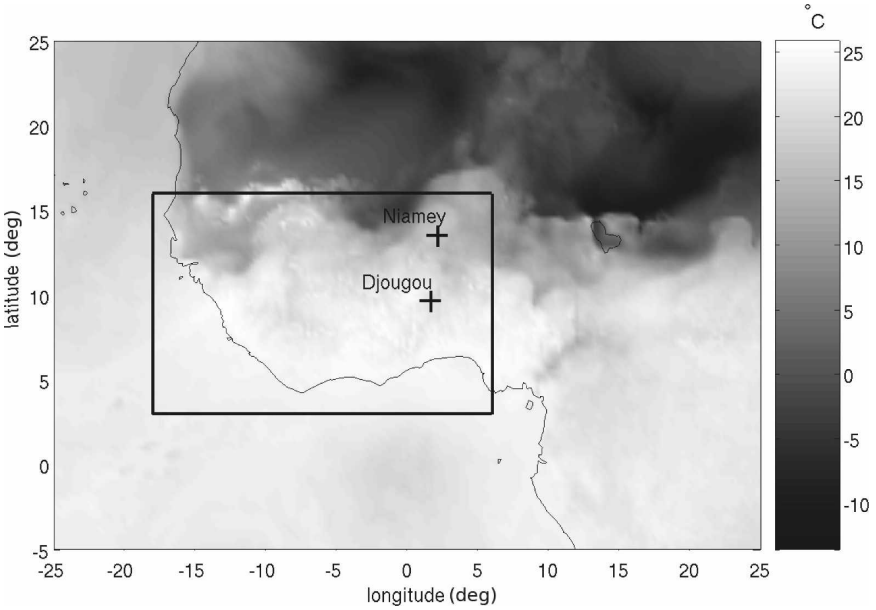

FIG. 1. ECMWF reanalysis of dewpoint temperature at the surface over West Africa and the Guinea Gulf, 0600 UTC 16 May 2006. The observations discussed in the article were obtained from instruments located near two towns indicated here: Niamey (Niger) and Djougou (Benin). The AMMA research domain is indicated by the black frame.

warm Saharan air layer (SAL) develops in the mean troposphere sloping up the monsoon layer. The conflict of these two air masses of different origin and thermodynamics takes place along the intertropical discontinuity (ITD) at low level and along the ITCZ in the midtroposphere.

Intimately related to the WAM system, three jets articulate its dynamic structure and impact on the convective activity (Thorncroft et al. 2003): the African easterly jet (AEJ) in the midtroposphere around 600–700 hPa (Burpee 1972; Thorncroft and Blackburn 1999; Parker et al. 2005a), the tropical easterly jet (TEJ) in the high troposphere around 200 hPa (Nicholson et al. 2007), and the subtropical westerly jet (STJ).

The work presented here deals with the diurnal variability of the low levels of the West Africa atmosphere and mainly focuses on another jet not listed above, which is the nocturnal low-level jet (NLLJ). The importance of this jet for the WAM was recently stressed by Parker et al. (2005b) using observations made during the JET2000 project (Thorncroft et al. 2003) and the Hydrological Atmospheric Pilot Experiment in the Sahel (HAPEX-Sahel; Goutorbe et al. 1997). Their study showed pilot sounding observations at the four main synoptic hours of the day during the 1992 wet season that revealed higher wind speed at 0600 UTC than at other times, with 10 m s^{-1} on average at 600-m height. In the conclusions of the recent workshop on monsoon climate system held in 2005 (Sperber and Yasunari 2006), the NLLJ is of paramount importance for any type of monsoon, not only because it transports humidity but also because it is related to numerous processes ranging from turbulence scale up to synoptic. According to Blackadar (1957) the formation of a nocturnal supergeostrophic jet follows the relaxation of the thermal turbulent friction force after sunset. In the absence of this frictional force (Persson 2002) the wind accelerates during the night and decelerates after sunrise with the development of turbulence. As the Coriolis force is weak in these low latitudes, the wind acceleration during the night is proportional and parallel to the horizontal pressure gradient force, which is linked itself to the temperature contrast and in particular to the Saharan heat low. This shows the importance of the heat low in the characteristics of the NLLJ. Using an idealized numerical simulation, Rácz and Smith (1999) were able to explain the observed diurnal cycle of low-level winds over Australia and the time delay between the heat low and the associated vortex. As the wind is negligible during daytime, the horizontal advection of humidity and also colder temperatures occur at night. During the day the turbulent mixing redistributes with height these quantities (Parker et al. 2005b). As a consequence rainfall intensity will be directly dependent on the NLLJ, which feeds the convective system.

As raised by Parker et al. (2005b), only a few analyses made before AMMA focused on the diurnal variability of the WAM, which is partly due to a lack of

high-frequency observations. About 50 yr ago, Farquharson (1939) and Solo (1950) emphasized diurnal changes in wind observed over West Africa. Hamilton and Archbold (1945) found similar results especially in the vicinity of the ITD. The HAPEX-Sahel experiment in 1992 (Goutorbe et al. 1997) gave the first extensive observational framework that allowed us to realize the importance of the WAM diurnal cycle. Using those datasets, Dolman et al. (1997) and Parker et al. (2005b) both stressed the importance of advection in the planetary boundary layer (PBL) budget in the Sahel during the night and the early morning. More recently, Sultan et al. (2007) characterized the diurnal cycle of the WAM around the monsoon onset based on reanalysis over 20-yr or 40-yr periods, and the interaction between the heat low activity, the NLLJ intensification, and deep convection. [Also, Peyrillé and Lafore (2007) studied the diurnal cycle of the WAM with a simplified 2D model and showed how it contributes to the moistening process for sustaining deep convection through nocturnal advection and daytime turbulent vertical transport.] The present study is a continuation of the works by Parker et al. (2005b) and Sultan et al. (2007) on the diurnal cycle of the WAM, with the benefit of the extended observational environment in space and time provided by the AMMA field campaign. In particular, it is the first time that wind profilers are deployed in Africa, to continuously observe the wind profiles within the mid- and low troposphere. Four UHF wind profilers were operated in four sites in Niger (Niamey), Benin (Nangatchori), Mali (Bamako), and Burkina Faso (Ouagadougou). Here we use the observations made by two of them, completed by radiosounding observations, to make the link with the water vapor diurnal cycle, and a ground station instrumented for turbulence measurements to study the impact of the NLLJ at the surface. Our objective is to give an overview of the presence and role of the NLLJ throughout 2006 and describe more thoroughly the diurnal cycle of the PBL during the transition period between the dry and wet season.

The experimental dataset and seasonal context are described in section 2. Section 3 highlights the importance of the diurnal cycle over 2006 in Niamey based on the radiosounding and wind profiler data, with statistics on the NLLJ. The impact of the NLLJ on the ground in Nangatchori is addressed in section 4 and finally section 5 focuses on the transition period between the dry and wet seasons.

2. Experimental data and seasonal context

Two different areas of close longitude are considered here (see Fig. 1): Niamey in southwest Niger (13°29′N, 2°10′E, 205 m MSL) and Nangatchori in central Benin (9°40′N, 1°40′E, 432 m MSL), about 450 km south of Niamey and 400 km north of the Guinean coast and close to the larger village of Djougou. The two areas significantly differ from each other, with an annual pluviometry of 1200 mm yr^{-1} in Benin versus 500 mm yr^{-1} in Niger. Because the wet season lasts much longer in Benin, the surface is more densely covered with vegetation (forest) whereas the area in Niamey has a large proportion of bare soil and tiger bushes.

a. Wind profilers

For the wind description of the lower atmosphere we use the observations of both the UHF wind profiler of the Atmospheric Radiation Measurement Program (ARM) facilities in Niamey during 2006 and of the UHF wind profiler of Météo-France at the supersite of Nangatchori. These two radars were operated on a continuous collection mode from 8 April 2006 until 14 November 2006 for the Nangatchori profiler with a long period of spare data and loss of sensitivity from 23 April to August 2006. The ARM profiler worked nearly without trouble between 4 April 2006 and 6 January 2007, except during an inactive period from 17 June to 2 July.

A UHF radar measures wind vertical profiles and backscattered signal strength between about 0.1 and 3–5 km depending on the conditions of the atmosphere. It operates by transmitting electromagnetic energy into the atmosphere and measuring the strength and frequency of the backscattered energy and can work in clear air or during precipitation events. In clear air the atmospheric signal is due to the backscattering by spatial irregularities of the air refractivity index at the scale of half the radar wavelength when the source of the fluctuations comes from a turbulent mixing that follows the behavior of the Kolmogorov inertial subrange. Air refractivity is a function of temperature and humidity; the latter dominates in the lower atmosphere. The conjunction of strong turbulence and acute mean vertical gradient of temperature and humidity produces the strongest echoes. This is the case at the top Z_i of the PBL, which is usually marked by a maximum of the refractive index structure coefficient C_{n^2} deduced from the radar reflectivity (Doviak and Zrnić 1993). This criterion is currently used to monitor the top of the PBL (Angevine et al. 1994).

The observation made by those two Doppler profilers was based on a repetitive sequence cycling over the five beams of about 5-min duration comprising a high and low collection mode. For the ARM radar the high mode observation starts at 330 m above ground with a radial resolution of 420 m, and for the low mode the

lowest observation level is 90 m and the radial resolution of 60 m. The Météo-France profiler uses a starting level of 150 m above the ground and a radial resolution of 375 m for the high mode, and for the low mode the lowest observation level is 75 m and the radial resolution 150 m. All the raw Doppler spectra are recorded and stored. This allows a reprocessing of the data to ameliorate the retrieval of the atmospheric parameters.

The same data processing (see Jacoby-Koaly et al. 2002 for details) is applied for both profilers. Vertical profiles of the wind are deduced from the Doppler spectra obtained at every level gate of the five radial directions for each cycle of measurements. For each meteorological peak selected from the Doppler spectra, the four first moments are computed, providing: the mean signal intensity (reflectivity), the mean Doppler radial velocity, the standard deviation (half the Doppler spectral width), and the skewness, a measure of the distribution asymmetry. The three wind components are deduced from the mean Doppler radial velocity measured on all beams with the assumption of local horizontal field homogeneity. The Doppler spectral width is specifically used to deduce the dissipation rate of turbulent kinetic energy (TKE) (Jacoby-Koaly et al. 2002).

b. *In situ measurements*

For the study of the profiles of the atmosphere above Niamey, we also use the data of the radiosoundings launched by the Agency for the Security of Aerian Navigation in Africa (ASECNA) 4 times a day during the whole year 2006. They were made at times close to 0000, 0600, 1200, and 1800 UTC (launches were often made 1.5 h or less before these times, but we use these notations in the text for the sake of clarity). The data were stored and processed by ARM.

In Nangatchori village, a ground station was operated by Laboratoire d'Aérologie from September 2005 to March 2007. As part of the AMMA Ouémé mesoscale site (Lebel et al. 2007, manuscript submitted to *Ann. Geophys.*), an 8-m-high meteorological tower was set up in a glade surrounded by secondary woodland, cultivated crops, and fallow that had been subjected to small-scale vegetation burning during the previous 5 yr. It lies within a southern Sudanian vegetation-type zone characterized by woodland savannah including the Isoberlinia species.

The equipment included full meteorological parameters, atmosphere composition (NOx, CO, O_3), and aerosols characteristics (absorption and diffusion coefficient, size distribution). Three-dimensional sonic anemometer and IR open path analyser (Licor 7500) measured temperature, 3D wind components, and humidity at 0.1-s time interval. The first-, second-, and third-order moments of the fluctuations were calculated with the eddy-correlation method over 30-min samples.

c. *Sequence of dry, wet, and transition periods in 2006*

For an entire year, Figs. 2 and 3 display the zonal component of the wind and the water vapor mixing ratio (WVMR) observed at Niamey and Nangatchori, respectively, and averaged over night or day, to highlight the diurnal variability. They allow us to clearly define at each latitude the dry and wet seasons during 2006 and the transition periods in between that we called "moistening" and "drying." Those four distinct periods are indicated at the bottom panel of each figure.

Note that we use the common criterion for detecting the monsoon flow used by Sultan and Janicot (2003), which is a positive zonal component (westerlies). The Harmattan associated with the dry period is characterized here by a negative zonal component.

The monsoon onset, which is the abrupt shift northward (at the climatological time and space scales) of the ITCZ in summer coming along with deep convection and rain in the Sahel, occurs at the end of the moistening period. Sultan and Janicot (2000) defined the onset as the period with a temporary decrease of convective activity along the ITCZ, before it increases again when the highest activity of the WAM sets. The onset period was found to be centered around 24 June on average between 1968 and 1990 and to last a couple of weeks. In 2006, Janicot and Sultan (2007) found this period of decreased activity of the ITCZ to be late relative to the average, extending from 25 June to 10 July and centered on 3 July. However, they also found that all the dynamic structures of the WAM were settled on time. Here, what we call the wet period in Niamey begins indeed at the end of this onset period. In Nangatchori, the wet season starts much sooner than the beginning of the onset transition.

In Niamey, the drying transition in October is sharp. On the contrary, the moistening transition at the end of April shows a slower moistening until mid-July.

In Nangatchori, the wet season is characterized by a very light positive zonal wind. It is much longer than the wet season in Niamey. This monsoon flow is associated with large WVMR of about 16 g kg^{-1}. The transition from wet to dry season lasts for 2 months, which is much slower than in Niamey. The dry season characterized by the predominance of Harmattan wind is particularly short, lasting for only 1 month. On the contrary, the moistening transition period from January to April is longer compared to Niamey. The transition

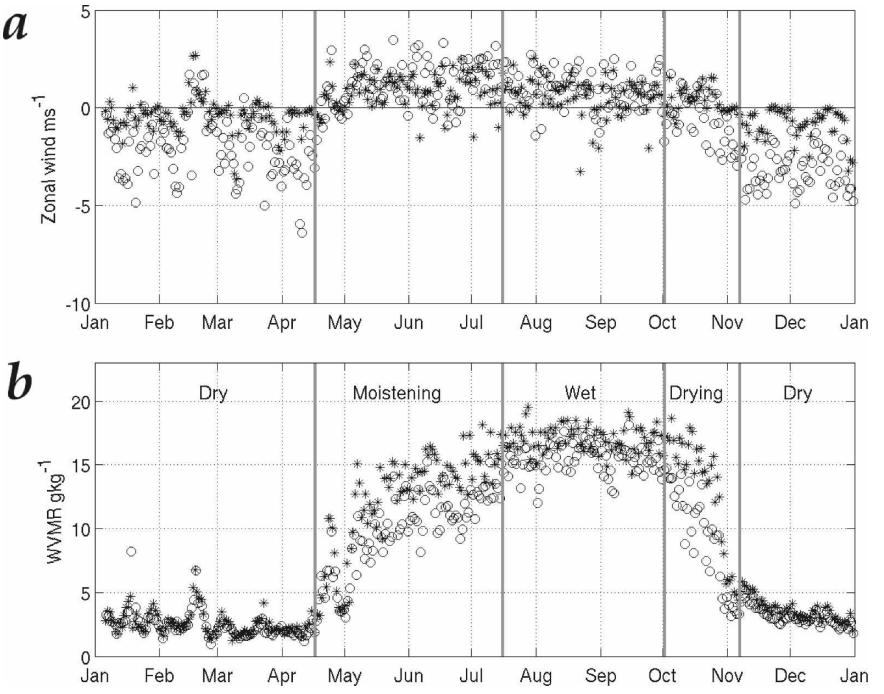

FIG. 2. (a) Zonal wind and (b) WVMR observed at the ground in Niamey during 2006, with nighttime average from 0000 to 0600 UTC (asterisks) and daytime average from 1100 to 1700 UTC (circles).

periods at both sites are associated with a strong signal of the diurnal cycle, which will be discussed further in the text.

It is known that the ITD migrates to the north in spring and to the south in autumn, following the apparent motion of the sun, like the ITCZ does (Sultan et al. 2007). Figure 4 shows the 6-hourly time series from April to October of the ITD latitudinal position at 2°E,

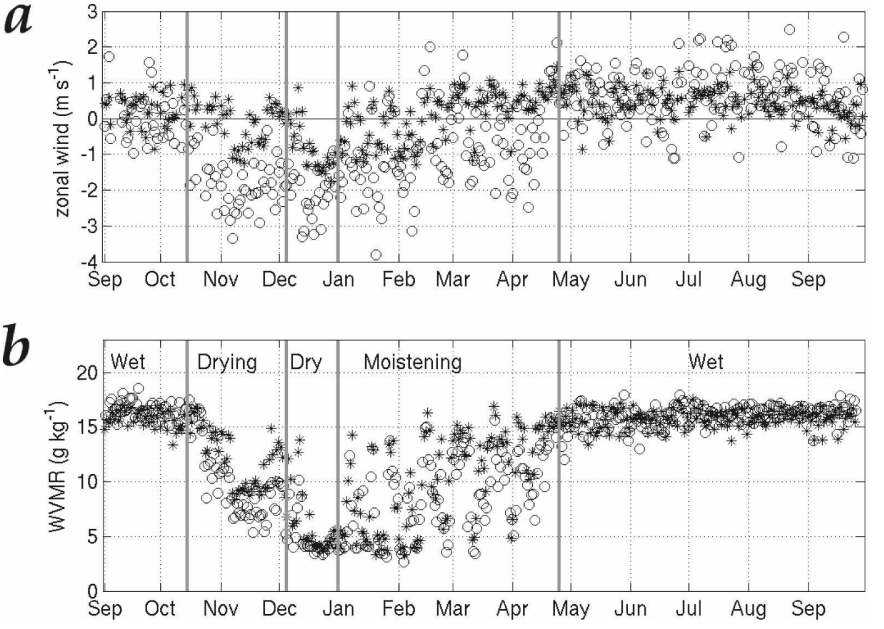

FIG. 3. (a) Zonal wind and (b) WVMR observed at the ground in Nangatchori from September 2005 to September 2006, with nighttime average from 0000 to 0600 UTC (asterisks) and daytime average from 1100 to 1700 UTC (circles).

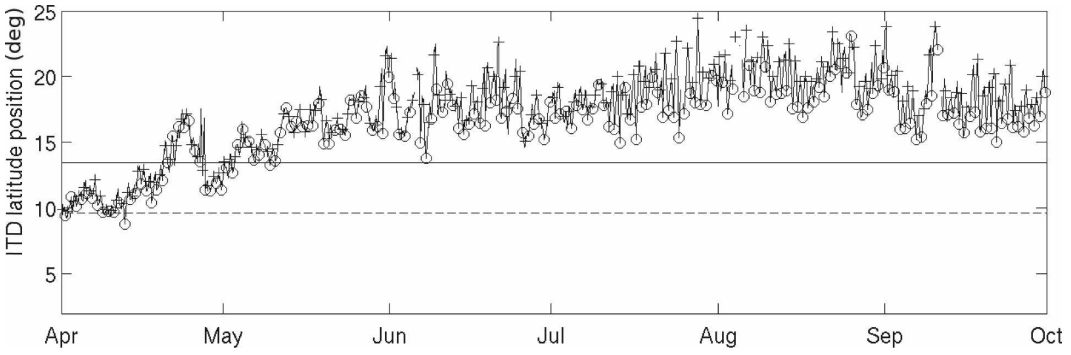

FIG. 4. Latitude position of the ITD at the longitude of Niamey from April to October 2006, based on surface dewpoint ECMWF analysis every 6 h [0600 UTC (plus signs) and 1800 UTC (circles)]. Solid and dashed lines show the latitude of Niamey and Nangatchori, respectively.

calculated from the European Centre for Medium-Range Weather Forecasts (ECMWF) analyses of dewpoint temperature at 2 m at 0.25° horizontal resolution (see Fig. 1). For a given longitude, the ITD position is determined from the dewpoint temperature field with the location of the maximum horizontal gradient of the dewpoint temperature. It shows that the ITD is still located at Nangatchori latitude in early April, but moves northward to reach Niamey latitude at the end of April and early May, which corresponds to the beginning of the moistening period mentioned previously.

3. Analysis of the diurnal cycle during 2006 in Niger

In this section, we give an overview of the diurnal cycle of the low troposphere during 2006 by use of the radiosoundings in Niamey, a statistical analysis of the wind profiler, and the ITD position and characteristics.

a. Radiosounding observations

The radiosounding observations at 6-h intervals give a picture of the diurnal cycle of the low troposphere over the whole year of 2006 at Niamey. Figures 5 and 6 display the monthly averages of horizontal wind (vector average), potential temperature, and WVMR at each of the four times: 0000, 0600, 1200, and 1800 UTC for 6 months of the year. The NLLJ is consistently observed every month. On average, it is already visible at midnight and 1.5–2 times stronger by 0600 UTC. Its maximum is located a few hundred meters above the ground. During the dry months, the WVMR remains around 3 g kg^{-1}, showing absolutely no diurnal cycle. The midtroposphere above (2000–4000 m) is even slightly less dry (around 5 g kg^{-1}), associated with the lower part of the STJ. In May, the STJ begins to migrate northward and the AEJ appears in the midtroposphere. For the following months until October, the entire mid- and upper troposphere is occupied by an easterly flow with wind speed reaching 14 m s^{-1} at 4000 m during the rainy season (July to September). The STJ comes back in the upper troposphere in October.

Unlike the very steadily dry low troposphere from January to April, a diurnal cycle of the WVMR is very well marked during the transition months of May and June, and especially in May. As seen for the wind, an increase in WVMR has already started at 0000 UTC in the lower troposphere, and continued until 0600 UTC with the WVMR maximum around 14 g kg^{-1} in May on average, compared with 9 g kg^{-1} at 1800 UTC. Later in the season, although the NLLJ still shows up from the monthly averages, there is no diurnal cycle of water because of more and more frequent rainy events and stronger impact of deep convection on the WVMR profiles, which are almost linear in the low troposphere. This simple analysis shows how transitional the month of May is in this area when the NLLJ begins to come from the southwest, with a strong supply of water vapor during the night followed by an efficient drying with daytime turbulent convection.

To characterize the NLLJ and its role in the northward transport of water vapor along the year, we consider for each radiosounding the (signed) maximum of the zonal component of the wind $u_{\max} = \text{sign}(u) \times \max|u|$ and the maximum of WVMR $r_{v_{\max}}$ in the lowest 1500 m of the troposphere. Both $u_{\max}$ and $r_{v_{\max}}$ are displayed as a function of time from January to October in Fig. 7. The times 0600 and 1800 UTC are distinguished by blue and red dots, respectively, and enable us to highlight the diurnal cycle. The change from dry easterlies to moist westerlies is very well seen in the top panel, with a transition in the last 15 days of April and early May. The NLLJ is put into evidence with maximum values of $|u_{\max}|$ at 0600 UTC 80% of the time in the dry season (estimate based on the period extending from early January to mid-April) and 66% of the ime

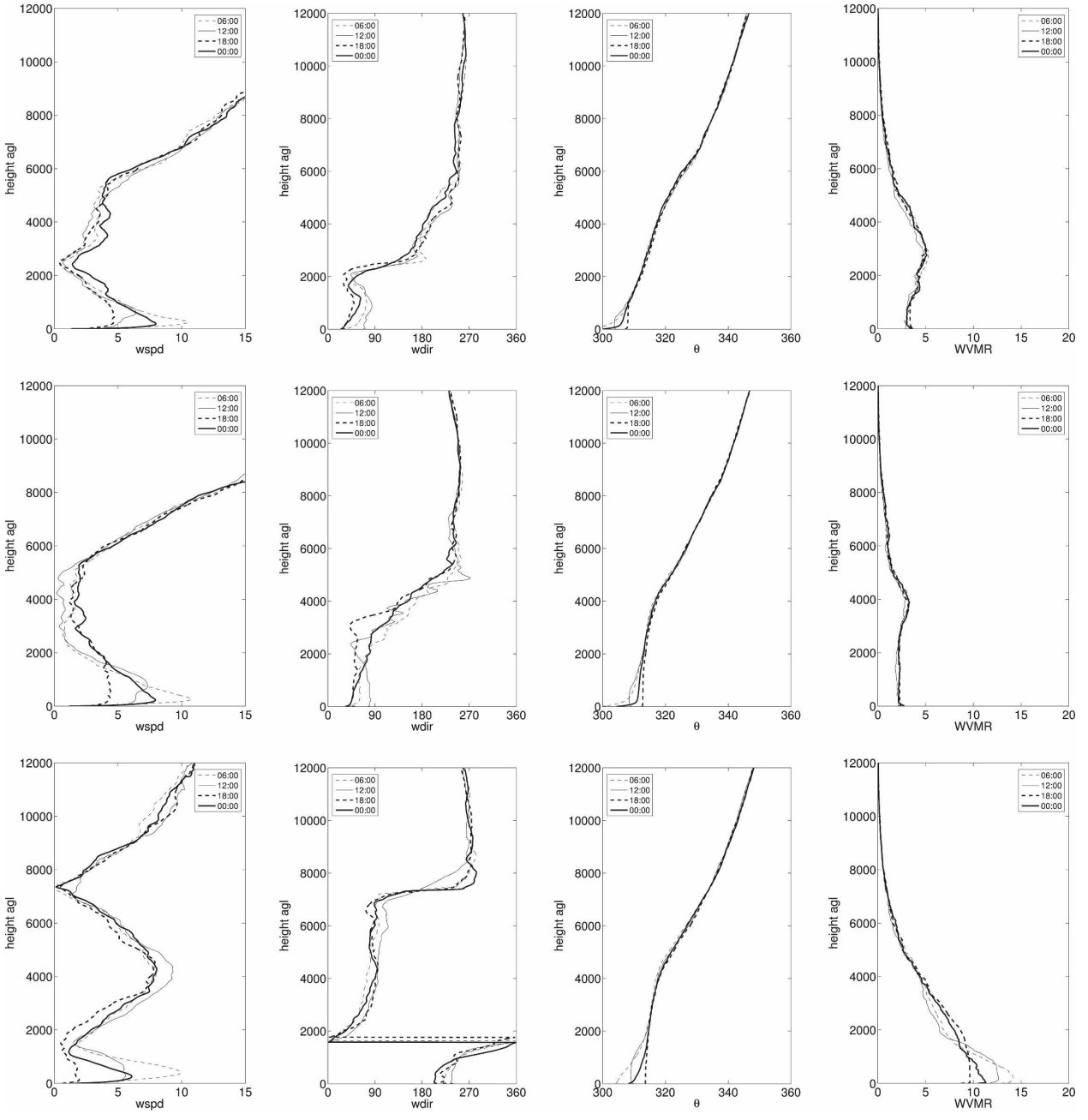

FIG. 5. Monthly averaged profiles for (top to bottom) January, March, and May of (left to right) wind speed, wind direction, potential temperature, and water vapor mixing ratio, observed by the radiosoundings over Niamey.

in the moistening and wet periods (estimate based on the period extending from the beginning of May to the end of September). The latter is more disturbed by the occurrence of deep convection, as testified by the daily cumulative precipitation displayed in Fig. 7b. The $r_{\upsilon_{\max}}$ time series show with more detail what was seen in the previous averaged profiles, especially the transition period in April/May characterized by the largest amplitudes of the diurnal cycle of WVMR.

The envelop of $r_{\upsilon_{max}}$ considered during the transition mentioned above, and extending over the last fortnight of April (see Fig. 7), is associated with the northward progression of the ITD across the area (see Fig. 4) and its temporary return to the south before it crosses the area again in early May. Afterward (wet season), $r_{\upsilon_{\max}}$ stays high as the ITD remains to the north until the end of October. During the moistening transition, as the ITD moves from south Niamey to north Niamey, the

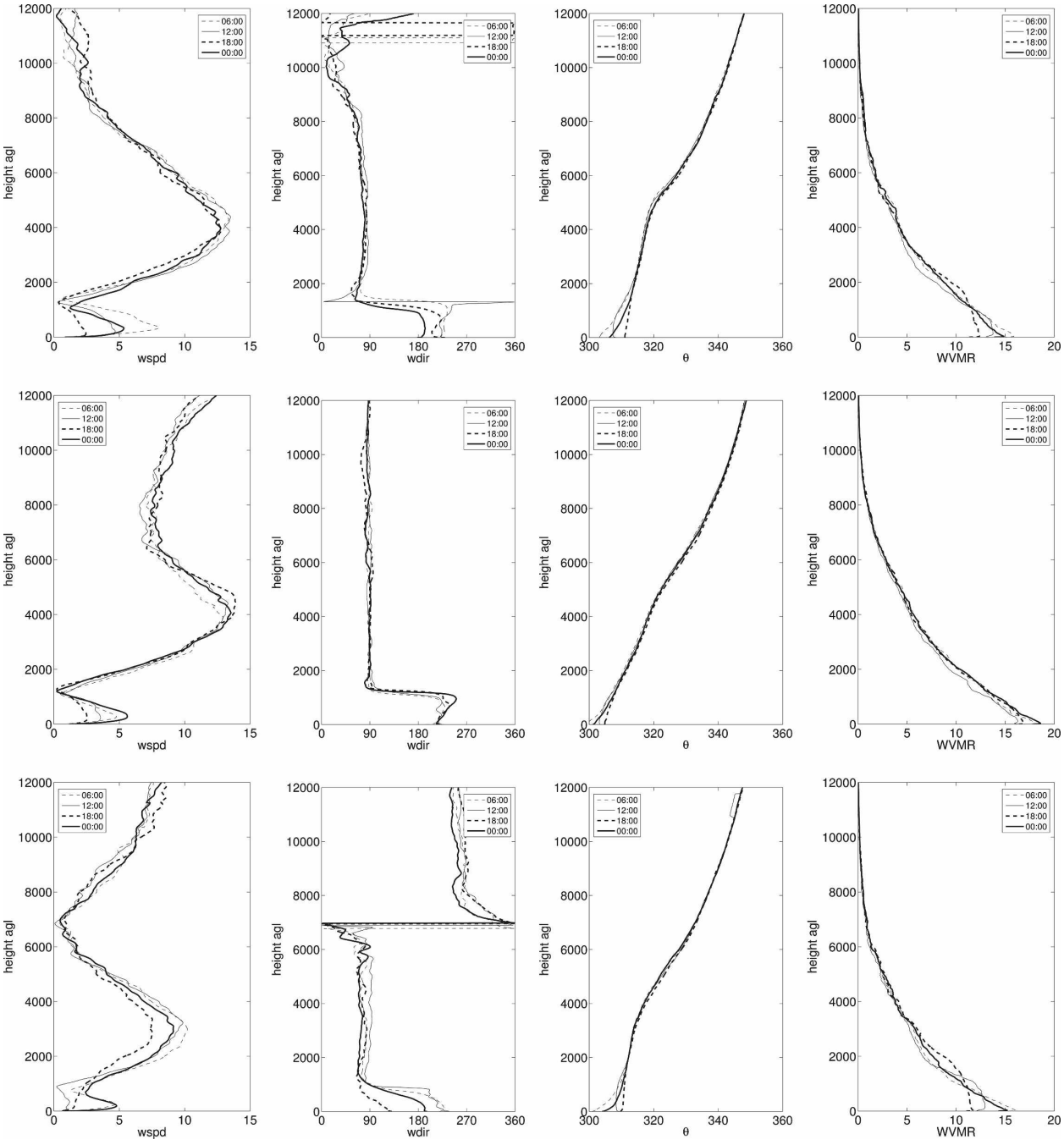

FIG. 6. Monthly averaged profiles for (top to bottom) June, August, and October of (left to right) wind speed, wind direction, potential temperature, and water vapor mixing ratio, observed by the radiosoundings over Niamey.

strongest $u_{\max}$ (NLLJ at 0600 UTC) veers from Harmattan (easterly component) when the whole troposphere is in the SAL (ITD to the south) to monsoon (westerly component) when the monsoon layer occupies the low troposphere (ITD to the north). This veering can actually occur over one diurnal cycle, because of the diurnal cycle of the ITD position itself, which explains the large amplitude of the oscillations of $r_{\upsilon_{\max}}$ at that time.

We can lend more support to the presence and role of the NLLJ and quantify the amplitude of the diurnal cycle by taking the difference between $u_{\max}$ $[r_{\upsilon_{\max}}]$ and u (r_{υ}) at 1500 m AGL: $\Delta u = u_{\max} - u(z = 1500)$ $[\Delta r_{\upsilon} = r_{\upsilon_{\max}} - r_{\upsilon}(z = 1500)]$, where z is the height above the

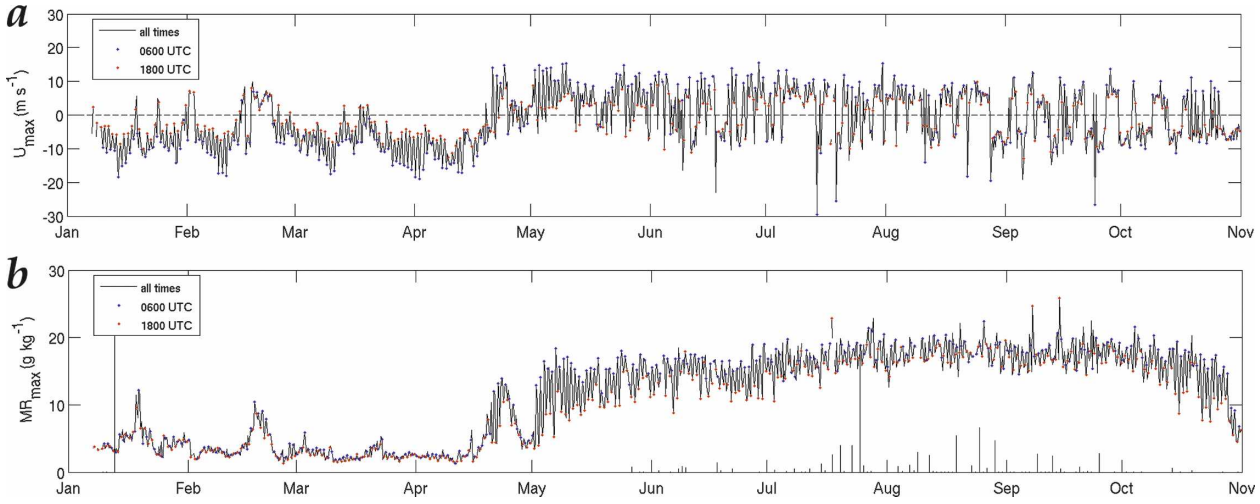

FIG. 7. The (a) u_{max} and (b) $r_{v_{max}}$ time series observed by the radiosoundings from January to October 2006 in Niamey. Blue and red dots indicate 0600 and 1800 UTC, respectively. Vertical black lines display the daily cumulative precipitation multiplied by ⅕ (mm).

ground. A strong Δu in the night denotes the presence of an NLLJ, while small values indicate that the vertical profile in the low troposphere is forced by other processes.

As found before, Δu and Δr_v are at a maximum at 0600 UTC most of the time (see blue dots in Fig. 8). The $|\Delta u|$ at 0600 UTC is around 10 m s^{-1} whatever the season, while Δr_v is less than 1 g kg^{-1} in the dry season, between 5 and 10 g kg^{-1} in the wet season, and up to 10 or 15 g kg^{-1} in the transition period. The change from a large amplitude diurnal cycle (from early May to mid-July) to a much weaker diurnal cycle afterward can be seen at the ground: it is marked in Fig. 2 by two different slopes of the stars (night average) and circles (day average) during that period. However, it is noticeable in Figs. 5 and 6 that the diurnal cycle at the surface has a very different signature than a few hundred meters above. This will be discussed further in section 4.

The seasonal variability of Δu and Δr_v at 1800 UTC (red dots in Fig. 8) tells more about the wet season setting. The Δu is usually weak at 1800 UTC, especially at the end of the dry season, when the increased solar radiation and dry soil enable a deep (much deeper than 1500 m), well-mixed PBL by that time. For the same reason, and also because of extremely dry soil and air already seen in Fig. 7, Δr_v is also very small. From the dynamical transition in early May to mid-July, Δr_v at 1800 UTC is getting stronger on average. This may be explained by the slightly moister PBL. The monsoon onset appears here as a shift of Δr_v at 1800 UTC to

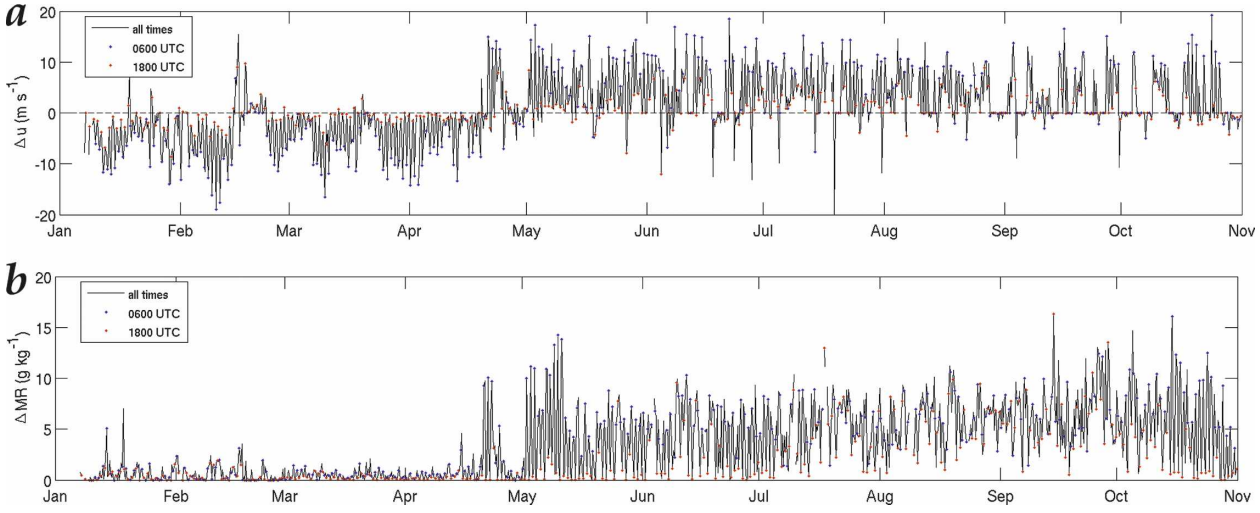

FIG. 8. The (a) Δu and (b) Δr_v time series observed by the radiosoundings from January to October 2006 in Niamey. Blue and red dots indicate 0600 and 1800 UTC, respectively.

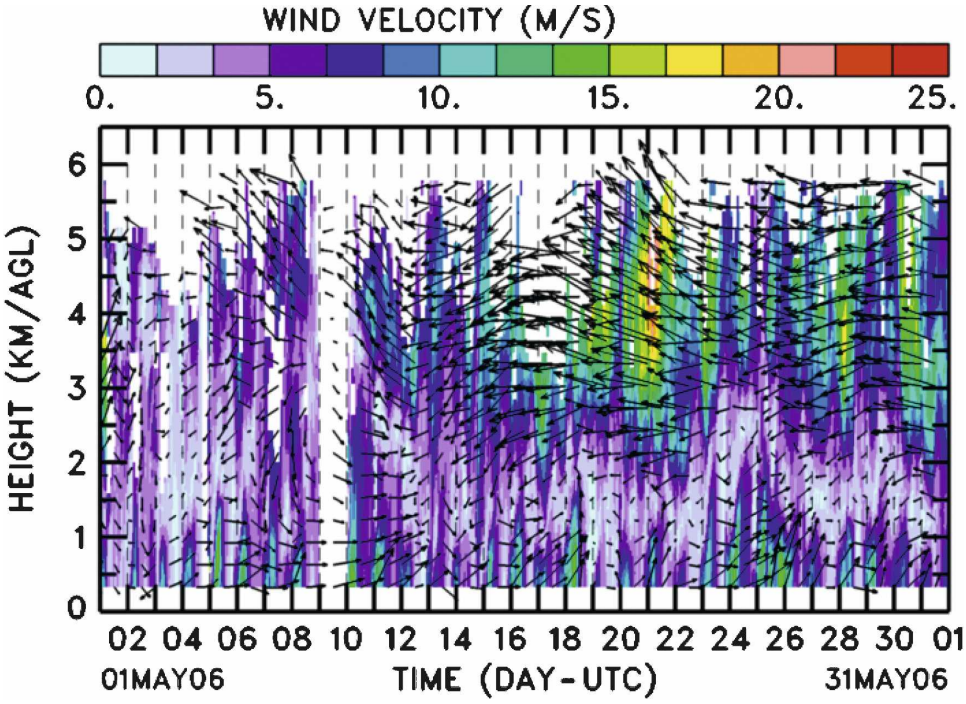

FIG. 9. Height–time cross section of horizontal wind (color scale is for wind speed) observed by the UHF wind profiler in Niamey during May 2006.

definitely larger values that almost never reach zero. This is due to a less-deep PBL, hardly reaching 1000-m depth, so that Δr_v and Δu at 1800 UTC often quantify the difference between the free troposphere and the underlying PBL.

b. *Statistic analysis of the nocturnal low-level jet based on UHF wind profiler measurements*

Figure 9 shows the observations of the UHF wind profiler in Niamey during May 2006. A jet clearly appears during the night and early morning in a repetitive pattern of strong southwesterly wind, reaching 10 to 15 m s^{-1} at about 500 m AGL, whereas the wind during the afternoon and evening is very light. The repetitious structure of the wind and reflectivity (or C_{n^2}, not shown) allows us to draw the composite image for this month in order to bring out the diurnal cycle. The composite image of both variables (Fig. 10) is obtained by averaging the observations over the whole month for each time of the day. The southerly component is found to peak at around 0600 UTC (10 m s^{-1}), with a vertical extent of the jet reaching 1200-m depth (Fig. 10a). The jet sets up in the evening at about 2000 UTC and decreases in the morning when the turbulence starts. It has entirely disappeared by 1200 UTC, when the mixing has reached the first 1500 m. The wind is very light in the PBL during the day, because of convective activity. The PBL depth, deduced from the reflectivity maximum, reaches 2300 m at 1500 UTC (Fig. 10b). The growth of the PBL is faster after 1200 UTC, when the jet has totally disappeared and the turbulence is purely thermal.

Similar observations of the UHF wind profiler in Niamey from April to December permit us to make statistics on the NLLJ occurrence with better temporal resolution (~15 min) than the radiosoundings allow. Figure 11 displays the distributions between April and December in Niamey of the maximal wind velocity, its time of occurrence, and its height above the ground. The time series of those characteristics are displayed in Fig. 12. (Note that the sampling in June and January is insufficient to be fully reliable.) Only nights with the occurrence of the NLLJ were considered in Figs. 11 and 12a–c. The criteria for the occurrence of the NLLJ (indicated in Fig. 12d) are defined from what was learned from the previous analysis of the radiosoundings, with (i) a wind maximum in the late evening or early morning that differs by at least 3 m s^{-1} from the 1800 UTC maximum wind and (ii) the position in height of this maximum below 1500 m AGL. Figure 11a shows that the maximum is centered around 0500 UTC with a standard deviation of 2.4 h, and a most probable time between 0600 and 0700 UTC. It is located at about 450 m AGL (with a most probable value smaller than this, around 350–400 m) and its maximum wind speed is 15 ± 3 m s^{-1}. From Fig. 12, we find that the NLLJ

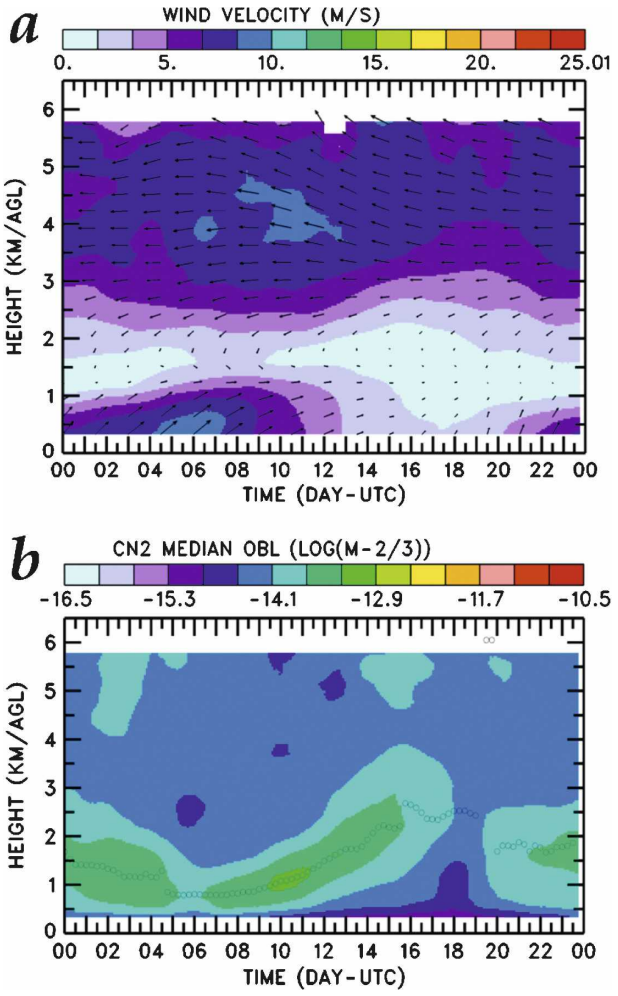

FIG. 10. Composite day based on Niamey wind profiler observations during May: (a) horizontal wind (color scale for wind speed), (b) C_n^2. Circles indicate the maximum of C_n^2 for each vertical profile, which during the day corresponds to the PBL top.

intensity decreases from the beginning of the moistening transition period (end of April) when it reaches 20 m s^{-1} to the end of the drying period (October) when it is only 10 m s^{-1}. It reaches higher values during the dry season. The percentage of occurrence of the NLLJ decreases from 85% in April to 52% in October and increases again to 90% and 97% in November and December, respectively. That is, the highest occurrence and strength of the NLLJ are observed during the dry season, when there is neither rain nor convective systems to disturb the setting of the jet during the night. The statistics relative to the time and level of the maximum wind speed are very steady during this season. During the whole period of westerlies in the low troposphere (i.e., when the ITD is located to the north of the Niamey area), the highest probability of observing the jet is in the beginning of that period (moistening period), when the ITD is the closest. The intensity of the NLLJ is also larger then than later in the wet season.

Those observations can be linked with the study of Sultan et al. (2007) based on the National Centers for Environmental Prediction–Department of Energy (NCEP–DOE) and the 40-yr ECMWF Re-Analysis (ERA-40), where a composite analysis showed that the NLLJ seen at 925 hPa is a major feature of the second mode, with higher wind speed just before the monsoon onset. Contrary to our one-point view from the Niamey site, this analysis allows them to show the latitudinal extension of the southwesterly or northeasterly jet, respectively, south and north of the ITD, depending on the time of the year (see their Fig. 3b). Because the monsoon NLLJ sets in between the ITD and the ITCZ, it shows a maximum at a certain latitude that is moving northward during the setting of the monsoon and southward during its recession. This is consistent with our observations at the fixed latitude of Niamey. However, the NLLJ found in the reanalyses never gets larger than 8 m s^{-1} because of the poor resolution over the vertical and the lack of observations, both preventing accurate study of the lower troposphere.

c. *Diurnal cycle of the ITD*

As we have seen previously, the seasonal variation of the NLLJ can be linked with the average evolution of the ITD position. In addition, the ITD position itself displays its own diurnal cycle (see Fig. 4), which is related to the diurnal cycles of the PBL and to the large-scale forcings (Miller et al. 2001). The ITD moves northward during the night and southward during the day, similar to the dryline in the Great Plains (Miller et al. 2001; Wen-Yih and Ching-Chi 1992) moving westward from the Bay of Mexico during the night and eastward from the Rocky Mountains during the day. This diurnal cycle of the ITD position was also found by the analysis of Sultan et al. (2007).

We can further describe the ITD structure and diurnal cycle by considering the dewpoint temperature gradient across the front. The jump in dewpoint temperature ΔT over 0.5° latitude across the ITD is shown in Fig. 13. It globally decreases from 20° to 30°C in April to about 5°C in September. The setting of the WAM (April–June) corresponds to the progression of a strong contrast across the ITD between the south side, which begins to moisten, and the north, which has been very dry for several months during the dry season. On the opposite end, the withdrawal (October) of the monsoon is associated with less contrast between areas that have both been moistened and watered during the wet season. The gradient observed is also in direct link with

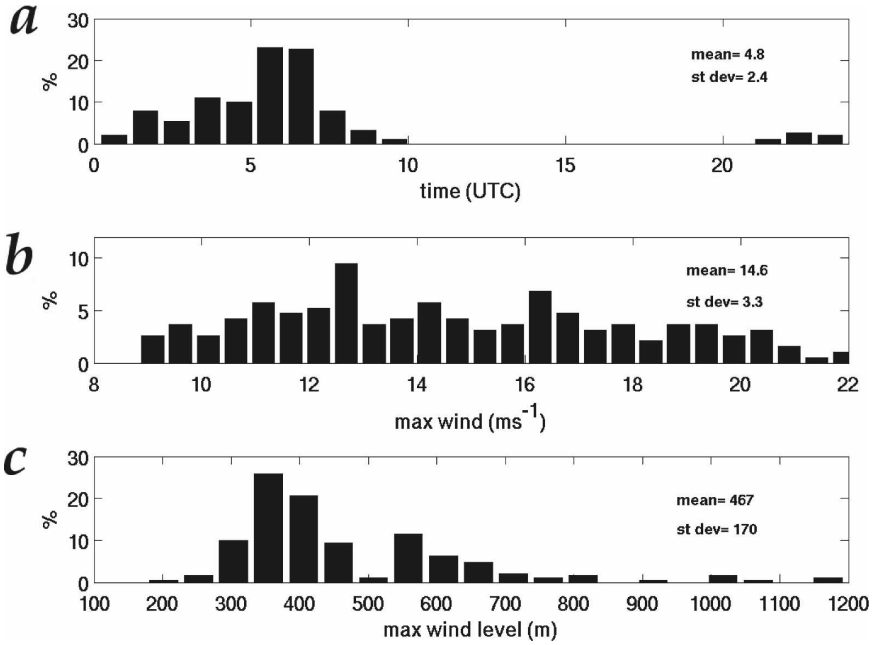

FIG. 11. Distribution of (a) the time of maximum speed of the NLLJ, (b) maximum wind speed, and (c) height AGL of the maximum wind speed, based on the UHF wind profiler observations at Niamey from April 2006 to January 2007.

the gradient of vegetation at the surface, which is the most pronounced between 9° and 14° of latitude, especially at the end of the dry season.

The strong diurnal cycle observed in April–May on this gradient across the ITD is related to the moistening period. From the point of view of a fixed point at the surface, this transition period depends on the latitude, because it corresponds to the passage of the ITD at that point. But a general moistening period can be defined as linked with the progression of the ITD northward. The gradient is stronger during the night, because of the large difference between the moist NLLJ and the Harmattan. During the day, mixing by convection makes the gradient across the ITD much smaller besides pushing the ITD to the south. This actually makes the position of the ITD difficult to evaluate and even define, so that the position of the ITD and gradient across have a large uncertainty during daytime and need to be considered with caution.

4. Impact of the NLLJ at the ground

In this section, we raise the question of how the NLLJ can be revealed at the surface and which dynamical, thermodynamical, or turbulent parameters are the more suitable for highlighting its effects near the ground. The first step is to determine the atmospheric parameters affected by the NLLJ. The average wind speed and WVMR are primarily investigated. Two ground-based stations' data, from Niamey and Nangatchori, are available to carry on this study over a seasonal cycle, but only the Nangatchori surface station has provided the turbulent measurements for the present study. So we mainly focus on the Nangatchori area in this section.

Figures 2 and 3 show that there is no obvious NLLJ observed at the ground in Niamey and Nangatchori, because the wind is usually weaker at night. In both sites, the wind speed is indeed most of the time smaller than 5 m s^{-1} during the day (1 or 2 m s^{-1} on average) and smaller than 2 m s^{-1} at night. This difference is not surprising because the wind speed in the surface layer is known to depend on $\log(z)$ and on stability conditions (Businger et al. 1971; Dyer 1974); unlike what happens within the mixed PBL, the wind is usually lighter under stable conditions (night) and stronger under unstable conditions (day), except when other factors are involved, like slopes that create katabatic flows in stable conditions, coastal breezes, and so on.

Therefore, we consider the turbulent variables rather than the mean wind to characterize the signature of the NLLJ at a smaller scale close to the surface. Figure 14 displays the TKE and the skewness of the air vertical velocity S_w (equal to the third-order moment normalized by the standard deviation) measured at the Nangatchori ground-based station at 0300 UTC from September 2005 to September 2006. According to Mahrt

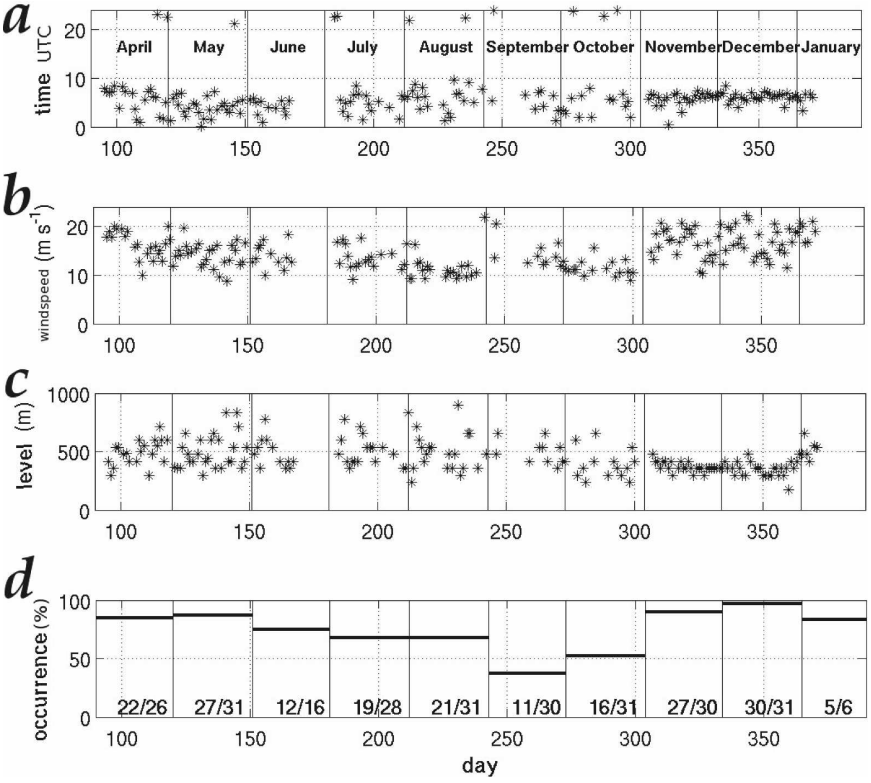

FIG. 12. Evolution from April 2006 to January 2007 of (a) the time of maximum speed of the NLLJ, (b) maximum wind speed, (c) the height of the maximum wind speed, and (d) the monthly frequency of occurrence of the NLLJ, based on the UHF wind profiler observations at Niamey. See text for criteria of occurrence and positioning of the jet. In (d), the ratio indicated for each month is the number of nights of NLLJ occurrence over the number of days with observation.

and Vickers (2002), the NLLJ develops in an "upside-down" PBL characterized by a source of turbulence aloft and a downward transport. The maximum wind speed of the NLLJ located at a few hundred meters AGL generates a wind shear that produces turbulence, in contrast with a more typical PBL for which the strongest shear is found close to surface.

The significant values of TKE observed during the night in Fig. 14 (except in November) confirm the occurrence of nighttime turbulence, and negative S_w as-

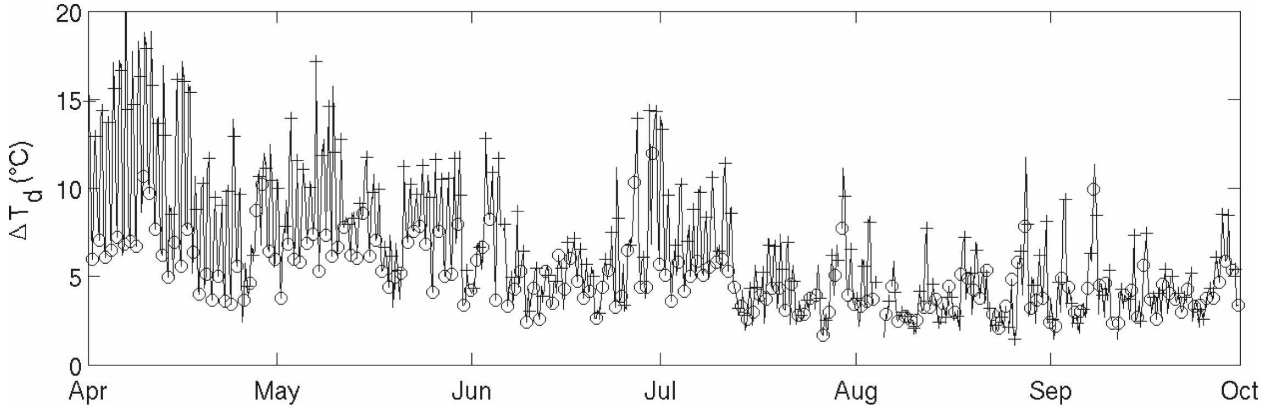

FIG. 13. Dewpoint temperature jump across the ITD over 0.5° latitude, at the longitude of Niamey from April to October, based on surface dewpoint ECMWF analysis. Circles indicate 0600 UTC and plus signs indicate 1800 UTC.

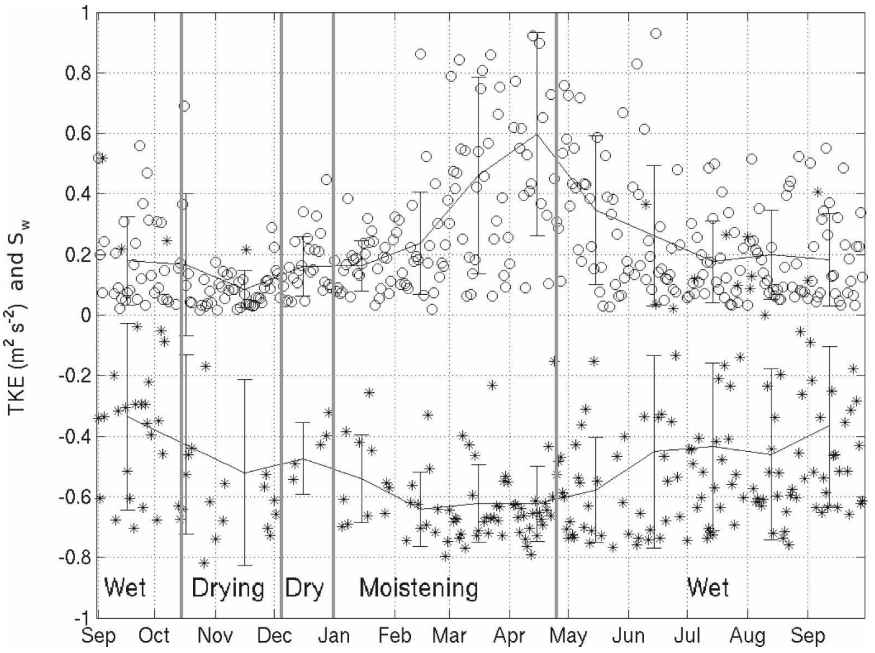

FIG. 14. TKE (circles) and skewness (asterisks) of the vertical wind component measured by the Nangatchori ground station at 0300 UTC from September 2005 to September 2006. Mean values and standard deviations are also indicated.

sociated with it attests to the downward transport of momentum. Although the variation along the year is more obvious on TKE, those two variables have a seasonal evolution and are anticorrelated: the larger the TKE near the surface, the larger the negative S_w. That is, the larger the turbulence observed near the ground during nighttime, the larger the downward transport that allows it to reach such a low level. Thus those two turbulent characteristics of the nocturnal stable PBL are likely to express the impact near the surface of an NLLJ located a few hundred meters aloft. In that way, the different periods identified previously in Fig. 3 can be found in the series shown in Fig. 14.

On average, the TKE and S_w are at a maximum during the moistening period. TKE scatter is the largest during this period because of some occasional very low absolute values of TKE. Probably no NLLJ settled during those nights or its intensity was not sufficiently large to have an impact close to the ground. In May and June, a progressive decrease of 50% of the mean absolute values of TKE and S_w is observed, while they remain constant during the rest of the wet season. The scatter is still large during the wet season because of some nights with large TKE and negative S_w that may attest to the presence of an NLLJ impacting down to the surface.

Thus, the TKE and S_w seem to be appropriate for detecting the NLLJ impact close to the ground. However, thresholds on TKE would be necessary to quantify the occurrence of the significant impact of the NLLJ close to the ground according to the time of the year.

One may attempt to link the turbulence intensity in the surface layer with the average dynamical condition. This is done in Fig. 15 where TKE values are plotted versus the zonal wind component at 0300 and 1500 UTC. According to this figure, the largest values of nighttime turbulence are observed for westerly winds, which means that the NLLJ affects the surface under monsoon flow preferentially. On the other hand, the turbulence associated with the NLLJ does not depend on the wind speed. The daytime observations (circles in Fig. 15) show an expected correlation between the TKE and the zonal wind intensity, and much more turbulence in Harmattan flow (clear and dry air) conditions. Note that in monsoon flow conditions, the TKE generated by the NLLJ can be as high as the daytime value.

For a further description of the diurnal cycle and the effects of the NLLJ at the surface depending on the time of the year, composite days of temperature, humidity, wind direction, S_w, and TKE are displayed in Fig. 16 for the periods mentioned previously: 1) the wet period (mid-April to mid-October), 2) the drying period (mid-October to early December), 3) the dry period (December), and 4) the moistening period (January to end of April), divided in two parts.

During the wet season, the monsoon flow is very weak (Figs. 16a,b), with a westerly wind of 1 m s^{-1}. The

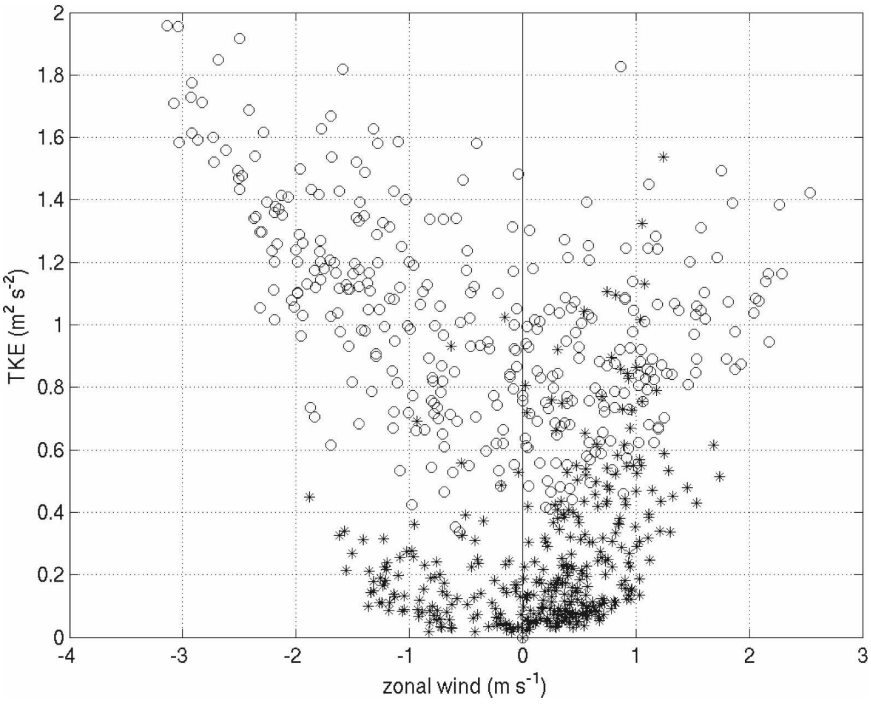

FIG. 15. TKE vs zonal wind at 0300:00 (asterisks) and 1500:00 UTC (circles).

WVMR remains constant during the entire day at 16 g kg^{-1} (Fig. 16c) and the temperature diurnal cycle is the least pronounced of the year, with a nighttime value of 23°C and a daytime value of 30°C (Fig. 16d). Also, S_w (Fig. 16f) remains negative during the day (unlike typical PBL), associated with disturbed conditions and likely rainfall events. The nighttime values are constant and quite large (−0.12) compared to the other periods of the year. The same observation can be made for the composite day of TKE (Fig. 16e), which does not show any maximum during the night but remains constant at 15% of its daytime value. This is difficult to justify because we expect a maximum of TKE during the night because of the effect of the NLLJ. At the same time, the nighttime values are quite large compared to the other seasons.

The drying period is characterized by a northeasterly to southeasterly flow of about 2.2 m s^{-1} maximum during the day. The air at the surface dried up from 16 to 10 g kg^{-1} but the WVMR has a specific diurnal cycle feature with moister air during the night (12 g kg^{-1}) than during the day (8 g kg^{-1}). This can be explained by the evapotranspiration of soil and vegetation confined in a thin layer during the night (the surface is still moist), leading to larger WVMR. The water vapor is then diluted during the day within the growing PBL and is also smaller because of the stomatal resistance to evaporation. The diurnal cycle of the air temperature is more pronounced during this period, with a larger cooling during the night and a larger warming during the day, because of clearer skies. The surface turbulence and convection induce a positive S_w during the day. At night, S_w is very small and TKE is smaller than 10% of its daytime value, as previously seen in Fig. 14. This drying period is certainly the least favorable for detecting the impact of the NLLJ at the surface.

During the dry season, the WVMR has a very small variation between night and day, as seen previously by use of the radiosoundings in Niamey. The WVMR is about 5–6 g kg^{-1} and the Harmattan flow speed reaches a 2.5 m s^{-1} maximum on average. The composite days of turbulent parameters highlight a weak downward transport of turbulence twice in the night, at 2200 and 0400 UTC.

According to the series shown in Fig. 3, the moistening transition period from January to April can be divided into two subperiods. It starts with an easterly wind, the ITD being on average to the south of Nangatchori. But the wind begins to turn to westerlies during a few nights between January and mid-February. For these nights, the WVMR jumps from 5 to 12 g kg^{-1}. During the second part of this transition, from mid-February to mid-April, a consistent oscillation is observed between westerly wind during the night (associated with WVMR larger than 15 g kg^{-1}) and easterly wind during the day (associated with WVMR ranging from 5 to 10 g kg^{-1}) because of the diurnal oscillation of the ITD with latitude. These features can be seen on

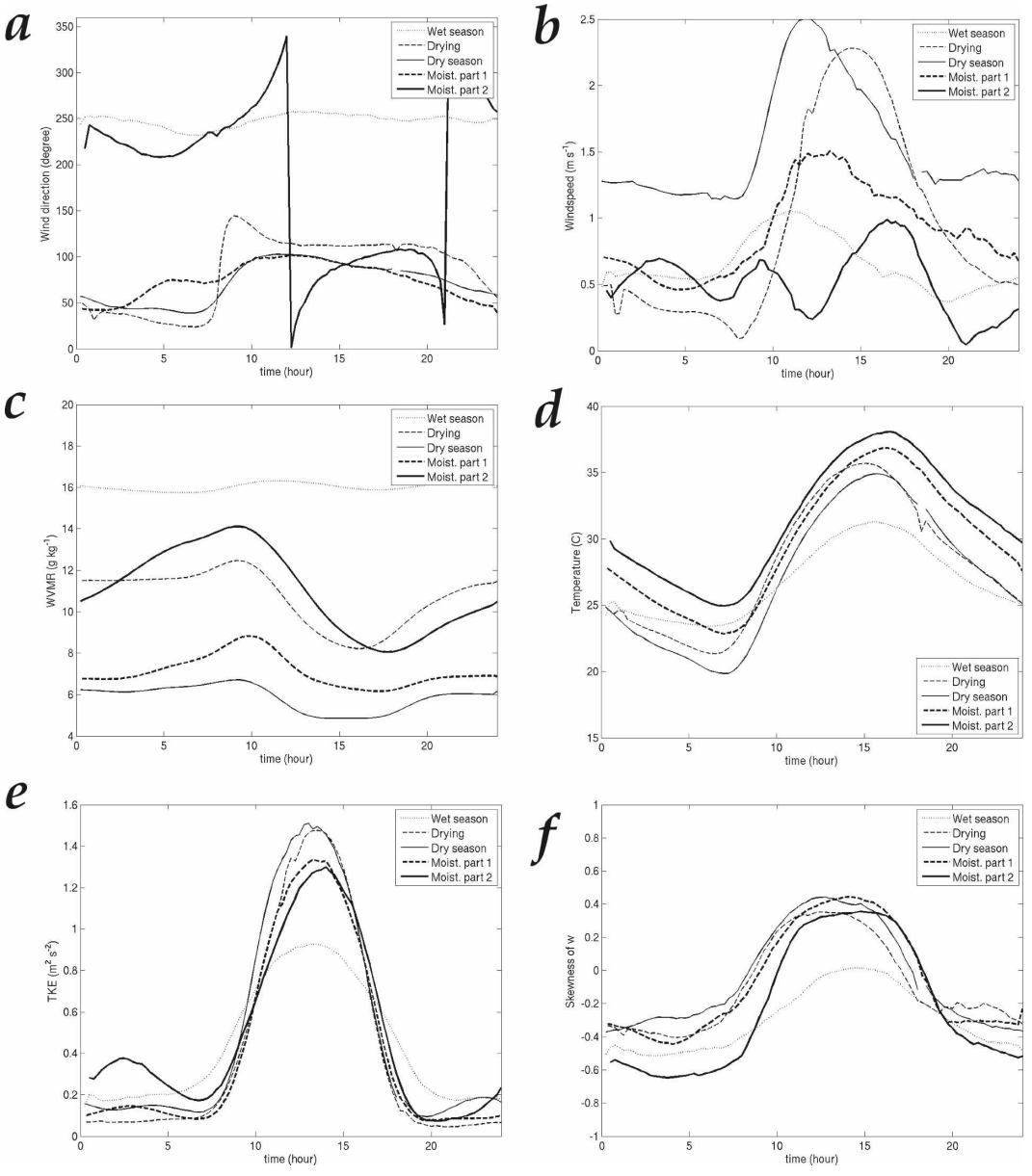

FIG. 16. Composite days for five periods of 2006 (see text for definition) observed at Nangatchori ground station: (a) wind direction, (b) wind speed, (c) water vapor mixing ratio, (d) temperature, (e) TKE, and (f) S_w.

the composite day shown in Fig. 16 for each of the moistening subperiods. According to this figure, the wind rotation is very slow, crossing north between 0800 and 1500 UTC. The Harmattan conditions settle at the surface for a 5-h short period until 2000 UTC. The wind speed composite day during the first part of the moistening period shows a traditional diurnal cycle with a maximum between 1100 and 1400 UTC. On the contrary, during the second part of the moistening period, the wind speed shows several maxima at 0300, 0900, and 1700 UTC. The first maximum is associated with the NLLJ impact at the surface, as will be shown in section 5. The increase of the wind starting around 0700 UTC is probably associated with the sunrise and the beginning of the PBL development. The change in the wind from the monsoon flow to the Harmattan flow generates a decrease of the wind speed. After 1230 UTC, with the ITD farther south, the wind speed increases again in Harmattan conditions generating the third maximum. Note that in Niamey, we found the surface wind maximum (of about 4 $\mathrm{m\,s^{-1}}$) usually around 0900 UTC (from a statistic analysis over the

whole year, not shown). This was also observed by Parker et al. (2005b) during HAPEX-Sahel and by May (1995) in Australia, and associated with the mixing down of the NLLJ. Even if the Harmattan flow endures at nighttime during the first part of the moistening period, the composite day of the WVMR highlights the start of the moistening with a more pronounced diurnal cycle than during the dry season and an increase of 2 g kg^{-1} on average. Because this moistening period ends before the first rainy event in Nangatchori (which occurs on 14 February), the WVMR increase cannot be related to the moistening of the soil and is likely due to advection with the NLLJ. This means that the few cases of nighttime westerly wind observed in Fig. 3b in January and February are not numerous enough to appear in the composite day of wind direction, but efficient enough to increase the average WVMR. Based on the turbulent parameters, we can check whether those cases of nighttime westerly wind are associated with an NLLJ or not. In fact, the TKE and S_w show a light downward turbulence with a maximum at 0200 UTC. This lends further support to the key role played by the NLLJ in the progressive moistening of the lower atmosphere during this period. Note that the increase in WVMR is maintained until 1000 UTC, that is a few hours after the NLLJ maximum, due to the mixing with the upper layers where the jet has set. The moistening is amplified by the arrival of the monsoon flow every night during the second part of the moistening period. At the same time, it is clearly the period with the largest nighttime turbulence, because S_w has negative values and the TKE shows a strong maximum (as high as 45% of the daytime maximum). Consequently, this period appears as that with the largest impact of the NLLJ on the surface.

In conclusion, the NLLJ effect on the surface is well highlighted by the TKE and S_w measured by a ground-based station. They indicate the existence of a primary source of turbulence in the low troposphere, and downward transport of turbulence down to the surface. Dynamical and thermodynamical surface characteristics allowed us to define four periods in the annual cycle during which the NLLJ has more or less influence near the ground. Westerly wind conditions seem more auspicious for observing the effect of the NLLJ near the surface but the occurrence needs to be quantified in a future study, by use of a TKE threshold, for instance. The higher occurrence of the NLLJ impact at the surface is observed during the moistening period characterized by a daily back-and-forth oscillation of the ITD position around Nangatchori latitude. The role of the NLLJ in moistening the low atmosphere is obvious then but also needs to be quantified more thoroughly. In the order of decreasing occurrence of NLLJ impact close to the ground, the wet season ranks after this moistening period, the dry season follows, and finally the drying period is the last.

5. Focus on the transition from dry to wet season

The analysis presented in the previous sections has highlighted the mean characteristics of the NLLJ and its evolution along the year, as well as its impact at the turbulence scale close to the ground. We found that the period when the role of the NLLJ is the most striking is the transition period from the dry to the wet season, which corresponds to the time when the ITD is located near the measurement area. This is in agreement with the study of Sultan et al. (2007) at global scale. The horizontal shift of the ITD during the day, with its most northern position around 0600 UTC (according to 6-hourly analyses), is thus directly linked with the alternation between Monsoon and Harmattan flows observed in the lower layers. The aim of the present section is to analyze more thoroughly the PBL diurnal cycle during this period, using the UHF wind profiler at both sites, completed with the radiosounding measurements in Niamey and the turbulence measurements in Nangatchori.

a. Transition in Niamey area

The NLLJ pattern is specifically shown in Fig. 17a for four consecutive days from 3 to 6 May 2006. The jet speed can reach 16 m s^{-1} at a level that climbs up with time in early morning. The marked presence of the NLLJ at 0600 UTC is confirmed by the radiosounding profile shown in Fig. 18 for 0600 UTC 3 May. This figure also displays the humidity mixing ratio and potential temperature between the surface and 6000 m AGL every 6 h. The low troposphere is well mixed at daytime as indicated by the temperature profiles and becomes 9 g kg^{-1} drier by 1800 UTC than earlier in the day. The PBL remains deep, well mixed, and dry at 2300 UTC, indicating that turbulent conditions were maintained late in the evening, maybe due to the aerosols found in the SAL that can slow down the nocturnal radiative cooling. In fact, the stable nocturnal layer visible at 0600 UTC 3 May seems to have set at low level shortly before 2300 UTC, because it has been observed only within the first 150 m AGL at 2300 UTC (not shown). The low troposphere has turned to stable conditions up to 1300 m between 2300 and 0600 UTC while the WVMR has reached 16 g kg^{-1}. The shear level between monsoon and Harmattan is located at 1300 m at 0600 UTC. This shear is associated with a transition

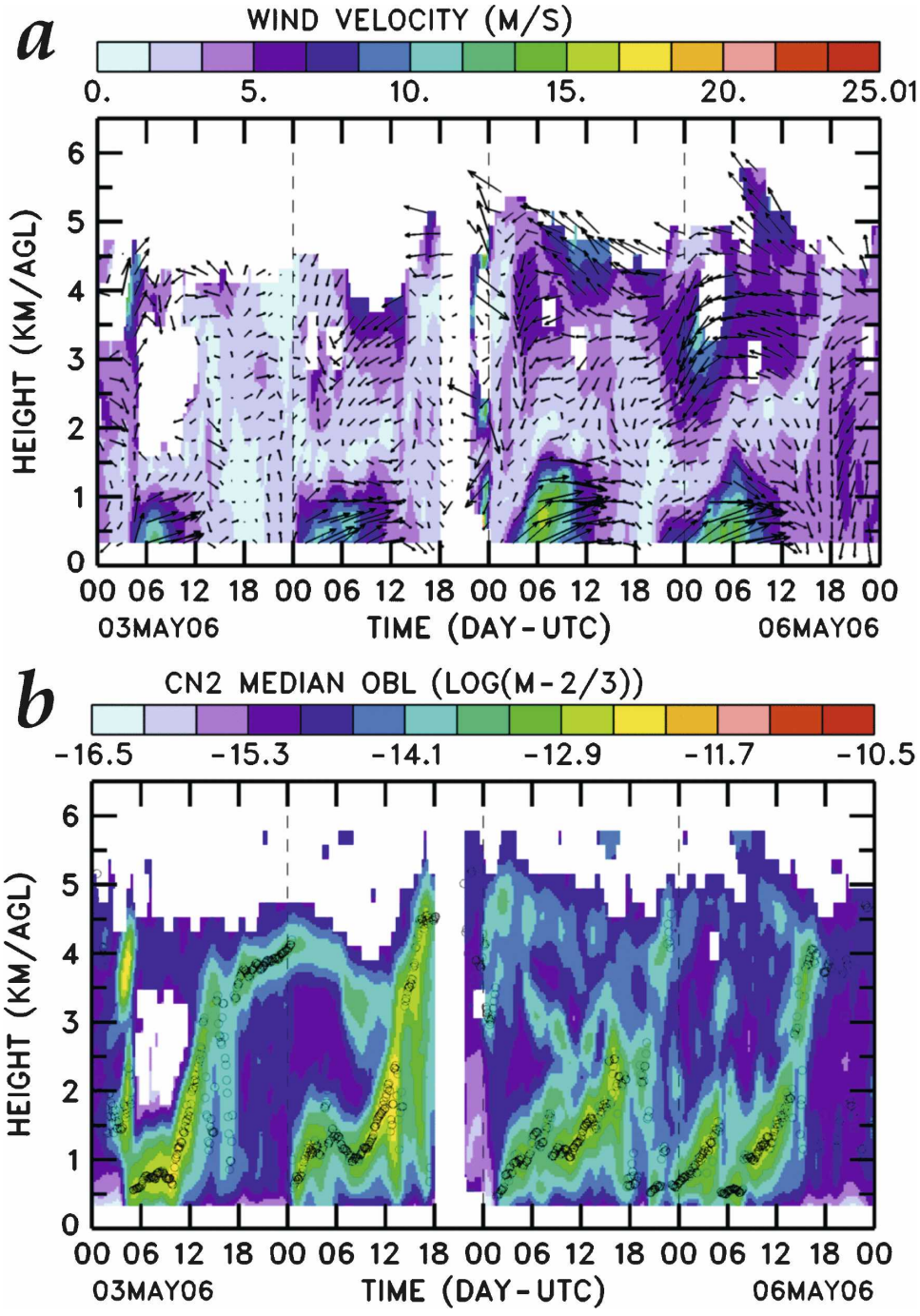

FIG. 17. Height–time cross section of (a) horizontal wind (color scale for wind speed) and (b) C_n^2 observed by the UHF wind profiler in Niamey during 3–6 May 2006.

in the temperature profile from stable to neutral and in the WVMR profile to a lower and more homogeneous value. This level also corresponds to a maximum in C_n^2 as can be seen in Fig. 17b. This, along with the positive slope of C_n^2 maximum in the early morning and the structure of the jet in time (Fig. 17a), enables us to suggest that the monsoon layer loaded with water vapor sets in with a thin tongue that deepens with time, likely in link with both the shape in space of the monsoon–Harmattan interface (the ITD) and the velocity of its progression northward. The advected air is cooler, moister, and less loaded with dust, which favors the

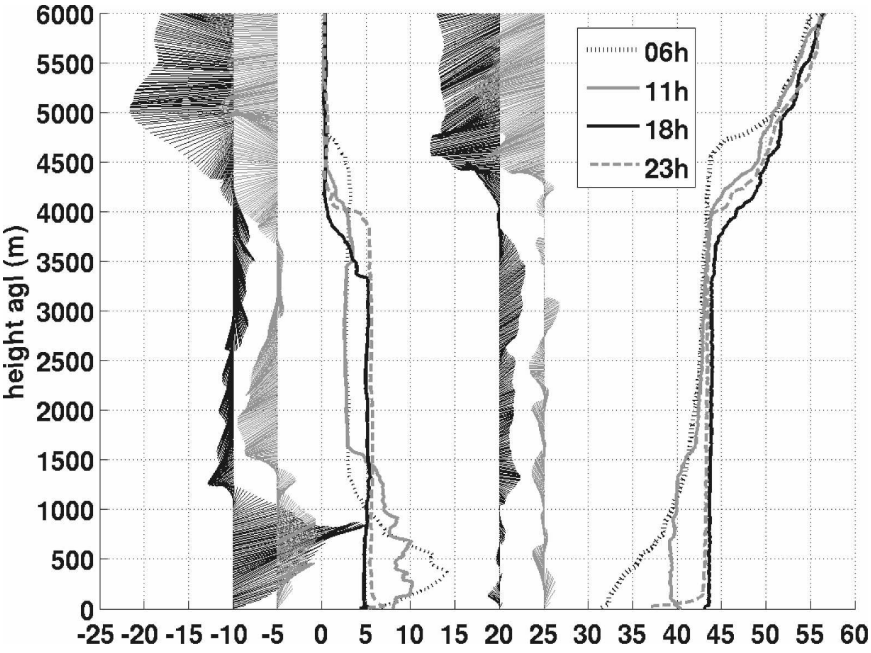

FIG. 18. Soundings observations in Niamey for 3 May 2006 at 0600 (black dotted line), 1100 (gray solid line), 1800 (black solid line), and 2300 (gray dashed line) UTC. (left to right) Wind vectors at 0600 and 1100 UTC, WVMR (g kg^{-1}) at all times, wind vectors at 1800 and 2300 UTC, and potential temperature (°C) at all times.

nocturnal radiative cooling. If we assume that during the night, the interface is moving at the same velocity of the observed wind, we find that its progression covers about 150 km within 6 h. This is entirely within the range of the diurnal amplitude found from the ECMWF analyses (see Fig. 4). However, one can imagine that the ITD does not move exactly at the speed of the observed wind, notably because of large-scale pressure forces.

According to the UHF wind profiler, the turbulence is the highest in the PBL after 1200 UTC, at the time when the jet has totally vanished (not shown). In fact, between 0600 and 1200 UTC, the turbulence grows and gradually destroys the jet. The wind turns very light and the monsoon flow is replaced by the Harmattan because of the mixing in the PBL (Fig. 17a). The PBL reaches 700 m at 1100 UTC and 3350 m at 1800 UTC (Figs. 17b, 18). The top of the residual layer can be seen around 4000 m on the morning of 4 May (Fig. 17b), which favors an even sharper growing of the PBL later on this day (up to 4500 m). Figure 18 also shows that the WVMR increases in the free troposphere between 1100 and 1800 UTC (from 3 to 5 g kg^{-1}), indicating a possible transport of humidity between the PBL and the SAL. Consistently, the WVMR decreases in the PBL, from 10 to 5 g kg^{-1} because of mixing within the PBL.

The radiosoundings enable us to make the link between the dynamics studied before and its impact on water vapor transport. Let us first note that a 12.5 m s^{-1} wind lasting for 10 h in the night can bring air (and water vapor) that comes from 450 km apart at the end of the night. The averaged profiles of May in Fig. 5 confirm the diurnal alternation at the scale of the month: the SAL gets moister along the day, while the lower troposphere dries. The convection within the PBL enables the exchange of water between the lower layers and the SAL and also dilutes the water vapor over a deeper layer. The opposite happens during the night: the Harmattan brings dry air in the midtroposphere while the NLLJ brings water vapor in the lowest stable layers. Figure 19a displays the average WVMR during April and May in the first 1500 m and the first 4500 m AGL, where the latter is approximately the height of the SAL inversion. It shows how the midtroposphere moistens during this transition, during two pulses of ITD northward, one at the end of April (18–25 April) and the second at the beginning of May (3–10 May). The strong diurnal cycle observed on the averaged WVMR over the first 1500 m during this transition is not so obvious on the averaged WVMR over the first 4500 m because the average is smaller in this deeper layer, and also because of the alternation explained above between nighttime advection by the NLLJ and daytime vertical transport through PBL processes. To

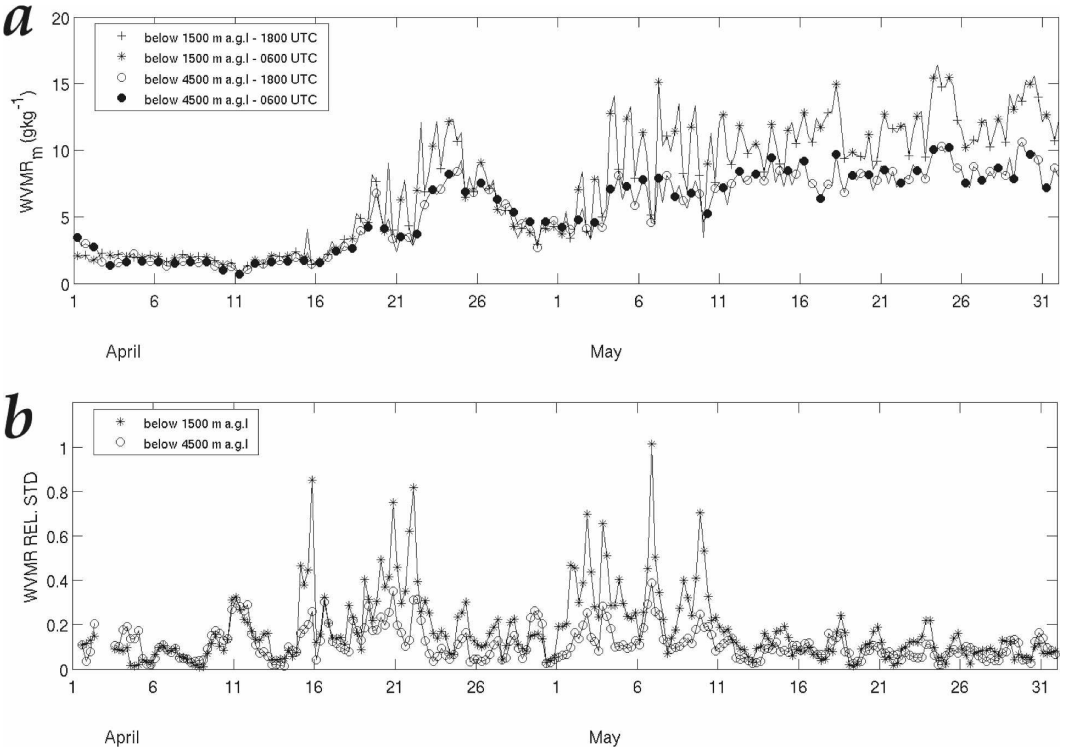

FIG. 19. (a) Time series from 1 Apr to 31 May of averaged WVMR over the first 1500 m (asterisks) and 4500 m (circles) AGL, and (b) relative 24-h standard deviation.

highlight the latter without trace of the first, Fig. 19b shows the standard deviation over 24 h in the same two layers, normalized by the mean. During the transition period, the relative standard deviation in the layer that is 1500 m deep can be 3 times larger than the standard deviation of WVMR in the first 4500 m, which includes both the CBL and the SAL, while they do not differ from each other before and after this specific period. If there was no transfer during that time from the low layer to the upper layer, one should see significant standard deviation of WVMR inside the 4500-m-deep layer too. This lends further support to the redistribution in the midtroposphere of the water vapor brought in the low layers during the night through the vertical mixing that occurs during the day within the PBL.

Thus, our observations with both radiosoundings and profilers suggest a large role played by the daytime convective turbulence in pushing the ITD southward, due to mixing, diluting, drying, and warming within the CBL. During the night the thin tongue of the NLLJ makes the ITD progress northward. This is in agreement with Jones and Bannon (2002) who found with a mixed layer model that the CBL heating is sufficient to drive a dryline and explain its diurnal variation. It is also confirmed by a horizontal gradient of the dewpoint temperature across the ITD that is much sharper at 0600 UTC than at 1800 UTC. Note that this is the opposite of what is observed in drylines, according to Schaefer (1986).

A more thorough study of those processes and numerical studies is required, similar to those made by Wen-Yih and Ching-Chi (1992), Miller et al. (2001), or Auslander and Bannon (2004) for the study of the diurnal variation of the dryline in the Great Plains, to estimate the part played by each process involved in the diurnal oscillation of the ITD and of its associated horizontal gradient, especially that played by the NLLJ.

b. Transition in Nangatchori area

Now we consider the equivalent transition period in the Nangatchori area. In Fig. 20, a focus is shown based on the observations by the UHF wind profiler during 4 days of April. The structure of the NLLJ is very different from that in Niamey: it sets up rapidly and uniformly with altitude and it is thinner (1000 m instead of 1500 m). It stops suddenly like in Niamey, but earlier. Thus, the description of the thin moist tongue brought by the jet in Niamey that deepens with time is not observed here. A thorough examination of the wind behavior at low level (not shown here) indicates that the NLLJ is preceded by a Harmattan jet (negative zonal

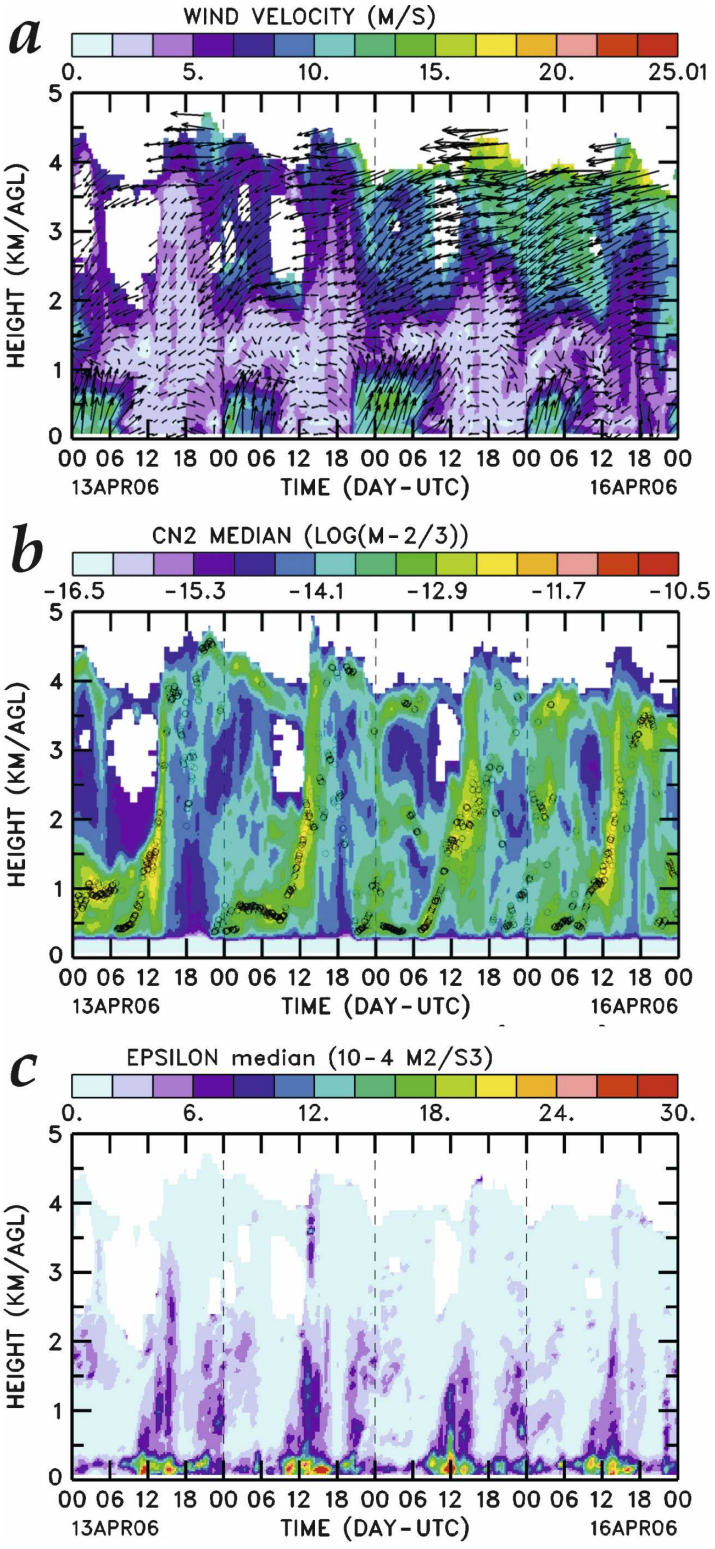

FIG. 20. Height–time cross section of (a) horizontal wind (color scale for wind speed), (b) C_n^2, and (c) TKE dissipation rate observed by the UHF wind profiler at Nangatchori during 13–16 May 2006.

component of the wind down to -6 m s^{-1} in Niamey and -10 m s^{-1} in Nangatchori). The difference is that the Harmattan weakens in Niamey before the monsoon jet sets up whereas it shifts instantaneously in Nangatchori from Harmattan to monsoon. This suggests that the ITD structure varies during its northward progression.

The repetitive peak that appears at night on C_{n^2} over Niamey is also present over Nangatchori. However, the maximum values are detected at a lower height in comparison to Niamey and in the immediate upper part of the jet. Some other relative maxima occur on 15 and 16 May around 2-km height: they correspond to the sharp gradient of humidity between the monsoon flow and the AEJ, which can reach 15 m s^{-1}. The residual layer can be observed during most mornings between 4.5- and 3.5-km height, showing a decrease in the PBL height that might be related to the AEJ subsidence from 14 to 16 May.

The turbulence detected by the UHF via the estimates of the TKE dissipation rate ϵ is consistent with the PBL development during the day. It varies between 3×10^{-3} m^{-2} s^{-3} near the ground to 10^{-3} m^{-2} s^{-3} at the PBL top. These significant values during daytime in the PBL are expected and associated with thermal turbulence. On the contrary, secondary maxima observed between 1900 and 0000 UTC depending on the day are less typical. They correspond to the front of the NLLJ when it sets up in the Nangatchori area, that is, to a rapid change in wind and moisture. The abrupt switch from easterly dry air to southwesterly wet air implies wind shear that may be favorable to dynamical turbulence in a 1.5- to 2-km vertical column. Also, shear-driven turbulence is still observed later within a 1-km-deep layer at the interface between the NLLJ and the overlying easterly flow.

In Fig. 21, the NLLJ intensity measured by the UHF wind profiler in Nangatchori from 11 to 21 April is compared with the conditions observed at the surface with the ground station. The jet intensity, the surface wind, and the TKE are correlated whereas S_w is not. All the correlation coefficients between these three parameters are larger than 0.85 for this 11-day period. As Banta et al. (2006) found, the ratio of the jet maximum speed to the TKE observed close to the ground is about 20 (21.5 here). TKE and $|S_w|$ both take large absolute values (TKE > 0.4 m^2 and $S_w < -0.6$), indicating significant turbulence and a "top-down" transport all along the period. The larger uncertainty on the estimates of skewness prevents us from bringing out a variation of S_w during this period. These results allowed us to highlight the consistency of NLLJ characteristics as detected by the UHF and its effects close to the surface. In future work, we plan to extend this analysis to a larger period and to the Niamey area to estimate a threshold value of TKE for detecting the NLLJ impact at the ground and point out favorable dynamical and thermodynamical conditions.

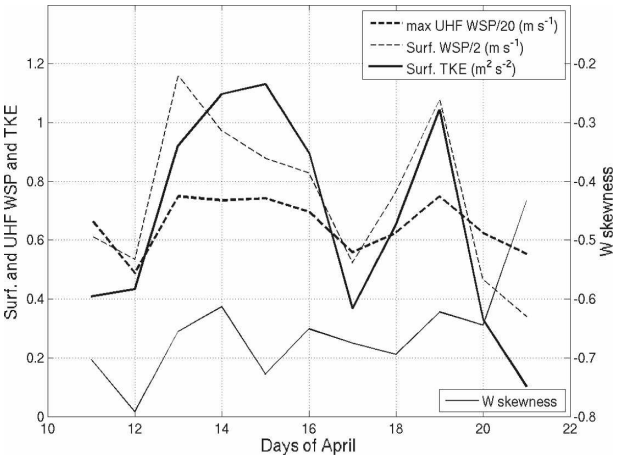

FIG. 21. Comparison between the maximal jet velocity observed with the UHF wind profiler and the surface characteristics in Nangatchori: maximal wind speed, TKE, and vertical velocity skewness. The wind velocities of maximal jet and at the surface are, respectively, divided by 20 and 2 for convenience.

6. Summary and prospectives

AMMA was the first field campaign during which wind profilers were operated in Africa, and this article shows the observations of two of the four wind profilers. As a starting point, we made here an overview of the diurnal cycle of the WAM during the AMMA SOP year of 2006 using integrative observations at two different sites in Niamey (Niger) and Nangatchori (Benin) that highlighted several key features and periods.

Our analysis of radiosoundings and UHF wind profiler measurements in Niamey confirm the assertion by Parker et al. (2005b) that radiosoundings at 0600 and 1800 UTC are crucial to picturing what happens in the lower troposphere in West Africa. The profiler measurements revealed a very consistent NLLJ all over the year, centered around 0500 UTC and 400 m AGL, with a larger occurrence during the dry and moistening periods (about 80% of the time) than during the wet season (about 60%). This jet comes either from the north or east during the dry season or from the south or west during the wet season, depending on where the ITD is located relative to the considered area. The high-resolution radiosoundings made in Niamey allowed us to emphasize the role of the NLLJ in bringing water vapor from the south during the night when the ITD

gets close to the area at the end of the dry season, and the role of the daytime PBL in mixing this water vapor within a larger depth of the troposphere. We think that the diurnal cycle of the PBL by itself can make the ITD migrate 1°–2° latitude during the moistening period.

During the transition from a dry to wet season, we find that the structure of the NLLJ in time and space is different between Nangatchori and Niamey, 450 km more to the north. This reveals the topography and evolution of the monsoon–Harmattan interface. The analysis of more extensive observations and the use of numerical simulation should help to describe and explain this structure. Also, it should be possible then to estimate the amount of water brought through advection by the NLLJ every night during the moistening period, and the amount of water that is incorporated in the higher troposphere through the exchanges at the monsoon–Harmattan interface during the day.

Similar to a dryline, the ITD is associated with an LLJ (monsoon flow) that is much stronger during the night (Sultan et al. 2007). But at the same time, in the very large, homogeneous, and flat plains of Africa, an NLLJ sets almost every night, even in an area that is far from the ITD, as we observed in our study. We need to better understand what makes those two kinds of LLJ different, because they merge somehow in the vicinity of the ITD—or rather, how the NLLJ is enhanced close to the ITD because of the strong thermal gradient across.

Based on the observations of turbulence made by a ground station, we find that the best signature of the NLLJ close to surface can be seen on the TKE and S_w, whereas there is no signature of the NLLJ on the mean wind. It is also the first time that those observations and analyses are made in Africa. Because we found several differences in the diurnal cycle and the seasonal sequencing between Niamey and Nangatchori, it should be interesting to figure out whether the signature of the NLLJ close to the ground found in Nangatchori remains similar in the Niamey area. The UHF wind profilers in both sites will enable us to go further in the description of the turbulence associated with the NLLJ.

Two other UHF profilers were operated in West Africa during AMMA, in Bamako (Mali) and Ouagadougou (Burkina Faso). The total of the four profilers should allow us to study the link between the AEJ and the NLLJ, because both jets can be seen by those radars. We also plan to do an analytical study of the NLLJ at those latitudes and compare with the observations, in particular to study the evolution with time and altitude of the wind speed and direction. Figures 17 and 20 show that the NLLJ wind turns slower to its right with time at Nangatchori than at Niamey, as we would expect when considering the larger Coriolis period in Nangatchori (70 h) than in Niamey (50 h). However, a more thorough study of this spatiotemporal structure, in both situations of geostrophic forcings (monsoon and Harmattan) and of the effect of the large Coriolis periods of those latitudes, would be worthwhile.

Acknowledgments. The authors of this work are funded by INSU-CNRS. Based on a French initiative, AMMA was built by an international scientific group and is currently funded by a large number of agencies, especially from France, the United Kingdom, the United States, and Africa. It has been the beneficiary of a major financial contribution from the European Community's Sixth Framework Research Programme. Detailed information on scientific coordination and funding is available on the AMMA International Web site (http://www.amma-international.org). We want to give special thanks to the cooperation of the U.S. Department of Energy as part of the Atmospheric Radiation Measurement Program for processing the sounding data of the Niamey site and for operating the UHF wind profiler in Niamey and providing the data. We thank Andreas Fink and Doug Parker for coordinating the radiosounding operation, and ASECNA for carrying it out. We are grateful to Sophie Bouffies-Cloche from IPSL for making available the ECMWF analyses. We also thank CNRM (Centre National de la Recherche Météorologique) at Météo-France for operating the UHF wind profiler in Nangatchori. Finally, we thank the reviewer for useful comments.

REFERENCES

Angevine, W. M., A. B. White, and S. K. Avery, 1994: Boundary-layer depth and entrainment zone characterization with a boundary-layer profiler. *Bound.-Layer Meteor.,* **68,** 375–385.

Auslander, G. M., and P. R. Bannon, 2004: Dryline bulge evolution in a two-dimensional mixed-layer model. *J. Atmos. Sci.,* **61,** 2528–2543.

Banta, R. M., Y. L. Pichugina, and W. A. Brewer, 2006: Turbulent velocity-variance profiles in the stable boundary layer generated by a nocturnal low-level jet. *J. Atmos. Sci.,* **63,** 2700–2719.

Blackadar, A. K., 1957: Boundary layer wind maxima and their significance for the growth of nocturnal inversions. *Bull. Amer. Meteor. Soc.,* **38,** 283–290.

Burpee, R. W., 1972: The origin and structure of easterly waves in the lower troposphere of North Africa. *J. Atmos. Sci.,* **29,** 77–90.

Businger, J. A., J. C. Wyngaard, Y. Izumi, and E. F. Bradley, 1971: Flux-profile relationships in the atmospheric surface layer. *J. Atmos. Sci.,* **28,** 181–189.

Dolman, A. J., A. D. Culf, and P. Bessemoulin, 1997: Observations of boundary layer development during the HAPEX-

Sahel intensive observation period. *J. Hydrol.,* **188–189,** 998–1016.

Doviak, R. J., and D. S. Zrnić, 1993: *Doppler Radar and Weather Observations.* 2nd ed. Academic Press, 562 pp.

Dyer, A. J., 1974: A review of flux-profile relationships. *Bound.-Layer Meteor.,* **7,** 363–372.

Farquharson, J. S., 1939: The diurnal variation of wind over tropical Africa. *Quart. J. Roy. Meteor. Soc.,* **65,** 65–180.

Goutorbe, J. P., A. J. Dolman, J. H. C. Gash, Y. H. Kerr, T. Lebel, S. D. Prince, and J. N. M. e. Stricker, 1997: *HAPEX-Sahel.* Elsevier, 1079 pp.

Hamilton, R. A., and J. W. Archbold, 1945: Meteorology of Nigeria and adjacent territory. *Quart. J. Roy. Meteor. Soc.,* **71,** 231–264.

Hastenrath, S., 1995: *Climate Dynamics of the Tropics.* Kluwer, 488 pp.

Jacoby-Koaly, S., B. Campistron, S. Bernard, B. Bénech, F. Girard-Ardhuin, and J. Dessens, 2002: Turbulent dissipation rate in the boundary layer via UHF wind profiler Doppler spectral width measurements. *Bound.-Layer Meteor.,* **103,** 361–389.

Janicot, S., and B. Sultan, 2007: The large-scale context of the West African Monsoon in 2006. *CLIVAR Exchanges,* No. 12, International CLIVAR Project Office, Southampton, United Kingdom, 11–17.

Jones, P. A., and P. R. Bannon, 2002: A mixed-layer model of the diurnal dryline. *J. Atmos. Sci.,* **59,** 2582–2593.

Mahrt, L., and D. Vickers, 2002: Contrasting vertical structures of nocturnal boundary layers. *Bound.-Layer Meteor.,* **105,** 351–363.

May, P. T., 1995: The Australian nocturnal jet and diurnal variations of boundary-layer winds over Mt. Isa in north-eastern Australia. *Quart. J. Roy. Meteor. Soc.,* **121,** 987–1003.

Miller, J., A. Thomas, and P. Bannon, 2001: A shallow-water model of the diurnal dryline. *J. Atmos. Sci.,* **58,** 3508–3524.

Nicholson, S. E., B. Some, and B. Kone, 2000: An analysis of recent rainfall conditions in West Africa including the rainy seasons of 1997 El Niño and the 1998 La Niña years. *J. Climate,* **13,** 2628–2640.

——, A. I. Barcilon, M. Challa, and J. Baum, 2007: Wave activity on the tropical easterly jet. *J. Atmos. Sci.,* **64,** 2756–2763.

Parker, D. J., C. D. Thorncroft, R. R. Burton, and A. Diongue, 2005a: Analysis of the African Easterly Jet using aircraft observations from the JET2000 experiment. *Quart. J. Roy. Meteor. Soc.,* **131,** 1461–1482.

——, and Coauthors, 2005b: The diurnal cycle of the West African Monsoon circulation. *Quart. J. Roy. Meteor. Soc.,* **131,** 2839–2860.

Persson, A., 2002: The Coriolis force and the nocturnal jet stream. *Weather,* **57,** 28–32.

Peyrillé, P., and J. P. Lafore, 2007: An idealized two-dimensional framework to study the West African monsoon. Part II: Large-scale advection and the diurnal cycle. *J. Atmos. Sci.,* **64,** 2783–2803.

Rácz, Z., and R. K. Smith, 1999: The dynamics of heat lows. *Quart. J. Roy. Meteor. Soc.,* **125,** 225–252.

Redelsperger, J., C. Thorncroft, A. Diedhiou, T. Lebel, D. J. Parker, and J. Polcher, 2006: African Monsoon Multidisciplinary Analysis (AMMA): An international research project and field campaign. *Bull. Amer. Meteor. Soc.,* **87,** 1739–1746.

——, and Coauthors, 2007: AMMA, une etude multidisciplinaire de la mousson ouest-africaine. *La Météorologie,* **54,** 22–32.

Schaefer, J. T., 1986: The dryline. *Mesoscale Meteorology and Forecasting,* P. Ray, Ed., Amer. Meteor. Soc., 549–570.

Solo, S. B., 1950: General circulation over the Anglo-Egyptian Sudan and adjacent regions. *Bull. Amer. Meteor. Soc.,* **31,** 85–94.

Sperber, K. R., and T. Yasunari, 2006: Workshop on monsoon climate systems: Toward better prediction of the monsoon. *Bull. Amer. Meteor. Soc.,* **87,** 1399–1403.

Sultan, B., and S. Janicot, 2000: Abrupt shift of the ITCZ over West Africa. *Geophys. Res. Lett.,* **27,** 3353–3356.

——, and ——, 2003: The West African monsoon dynamics. Part II: The "preonset" and the "onset" of the summer monsoon. *J. Climate,* **16,** 3407–3427.

——, ——, and P. Drobinski, 2007: Characterization of the diurnal cycle of the West African monsoon around the monsoon onset. *J. Climate,* **20,** 4014–4032.

Thorncroft, C. D., and M. Blackburn, 1999: Maintenance of the African easterly jet. *Quart. J. Roy. Meteor. Soc.,* **125,** 763–786.

——, and Coauthors, 2003: The JET2000 project: Aircraft observations of the African easterly jet and African easterly waves. *Bull. Amer. Meteor. Soc.,* **84,** 337–351.

Wen-Yih, S., and W. Ching-Chi, 1992: Formation and diurnal variation of the dryline. *J. Atmos. Sci.,* **49,** 1606–1619.